Dark matter substructures in electron recoil direct detection experiments

Tarak Nath Maity

Based on:

TNM R Laha; 2208.14471 to appear in JHEP

Advances in Astroparticle Physics and Cosmology

(AAPCOS-2023)

Dark Matter exists!

Dark Matter exists!

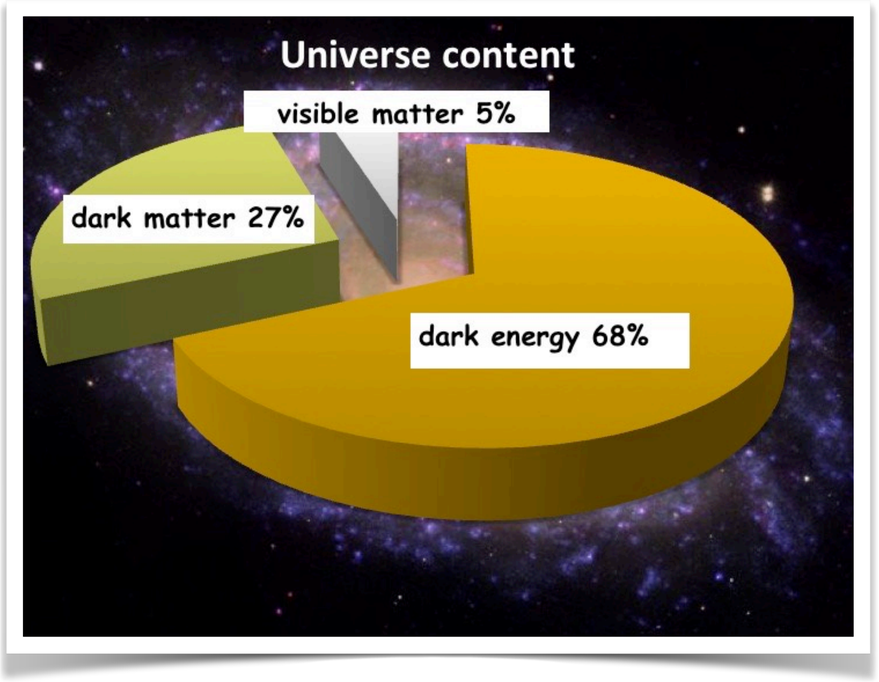

Image credit: QUANTUM DIARIES

Dark Matter exists!

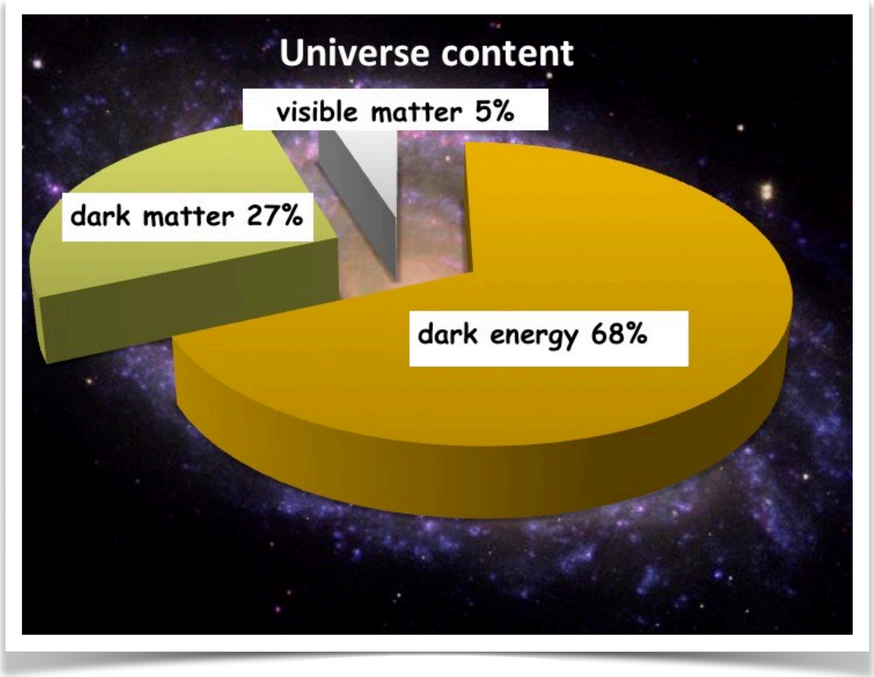

Image credit: QUANTUM DIARIES

- ☑ Stable: No decay, very long-lived
- ☑ Cold: Non-relativistic
- ☑ Massive: Wide range

Dark Matter exists!

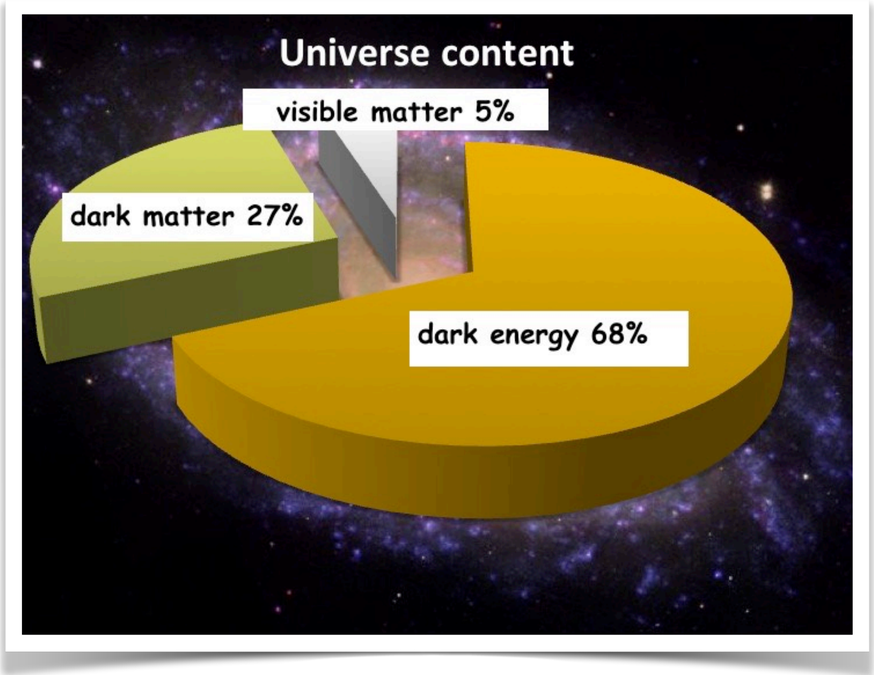

- ☑ Stable: No decay, very long-lived
- ☑ Cold: Non-relativistic
- ☑ Massive: Wide range

Image credit: QUANTUM DIARIES

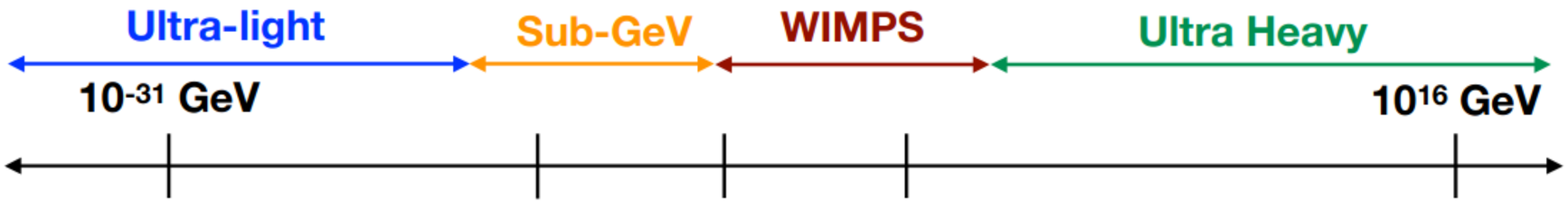

What else!

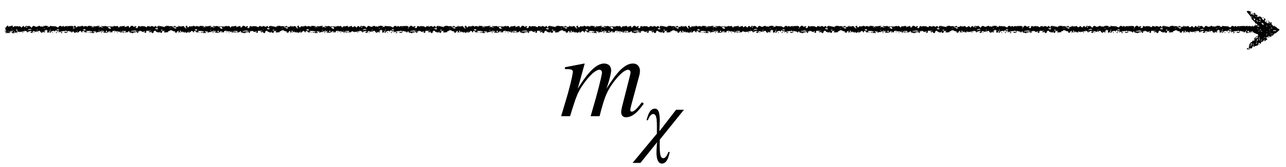

What else!

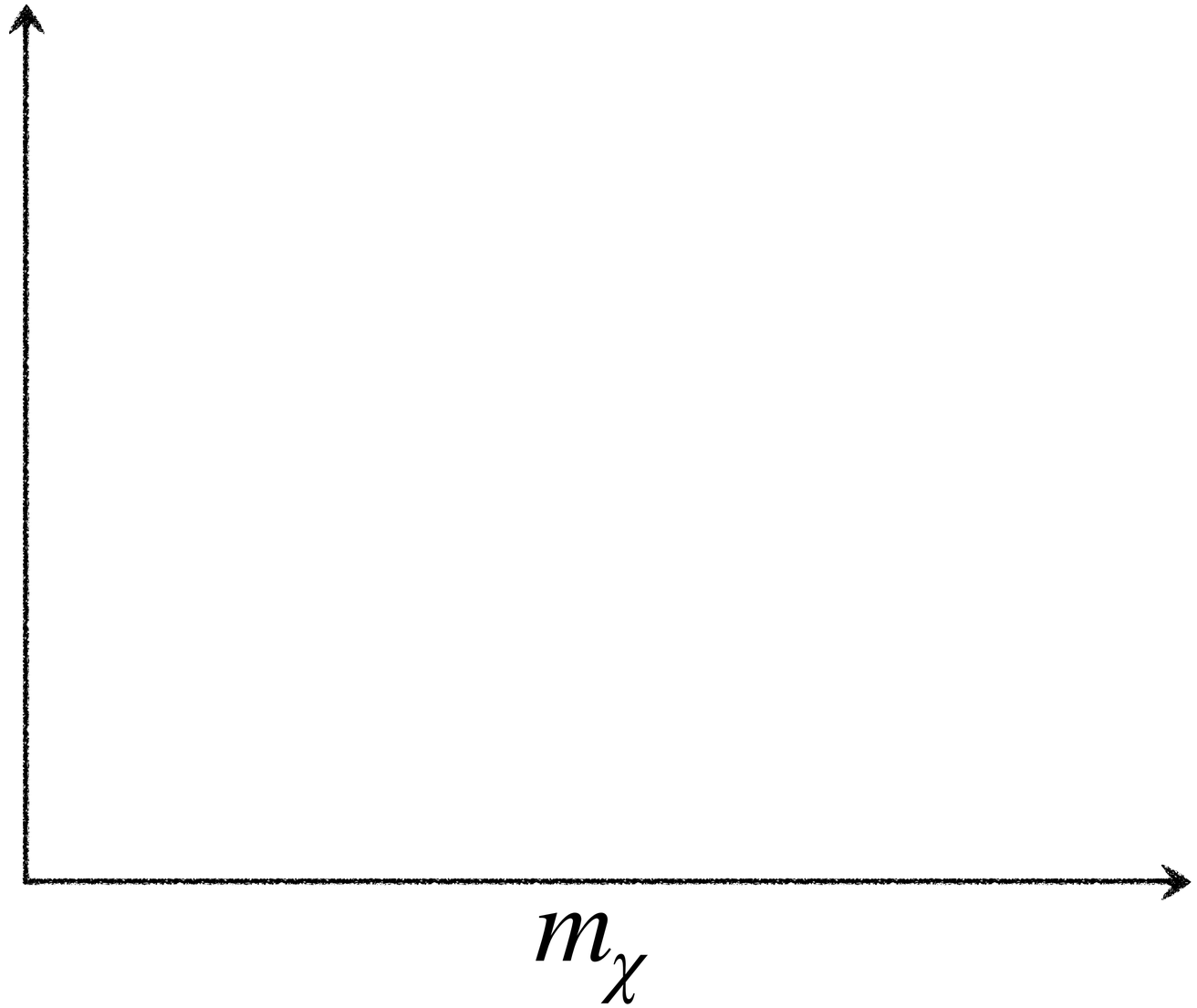

What else!

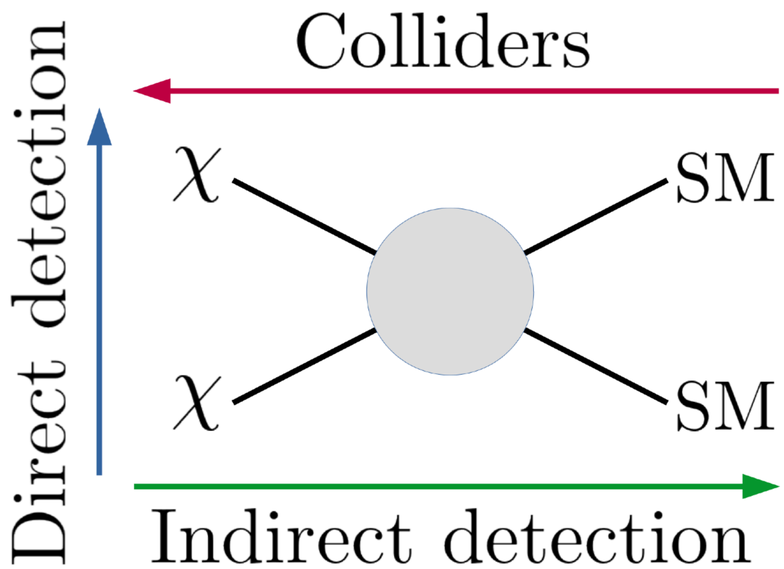
Colliders
Direct detection
χ
SM
χ
SM
Indirect detection

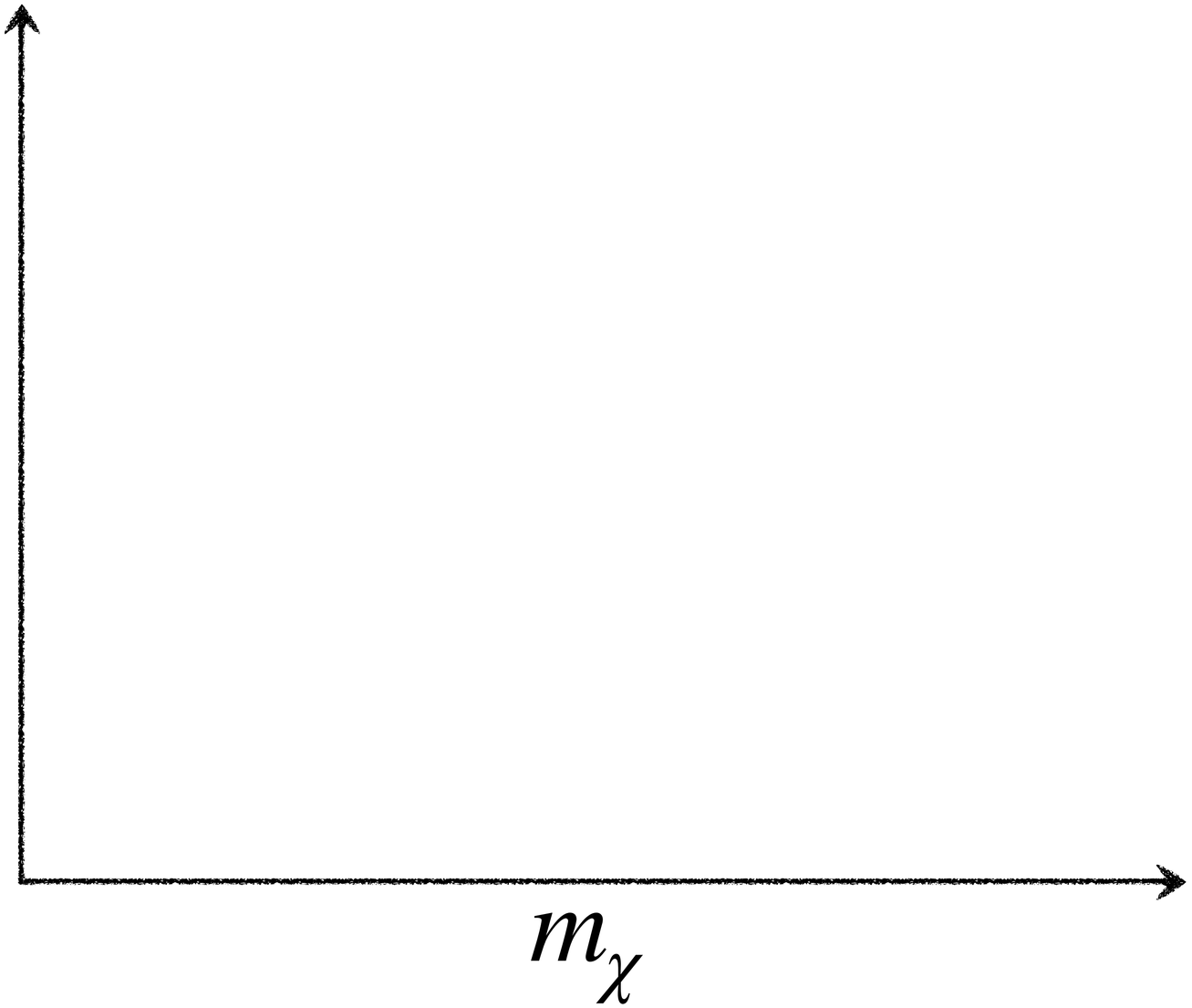
m_χ

What else!

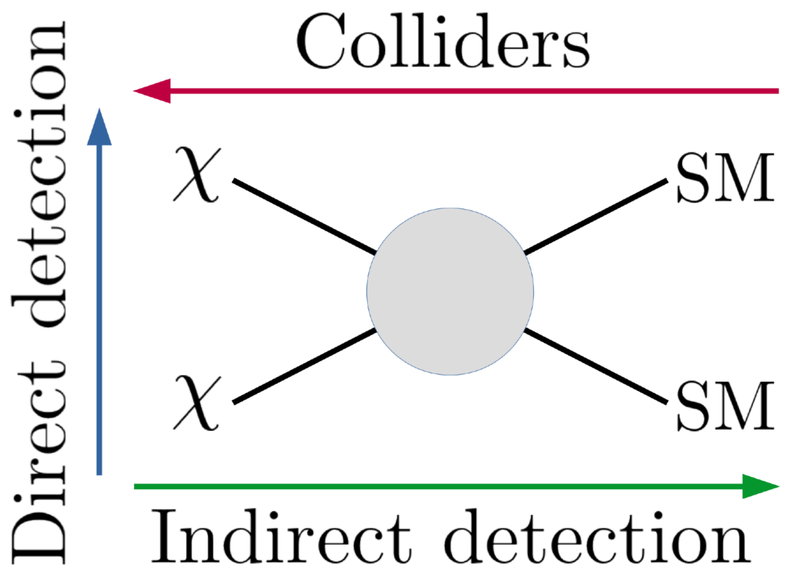

Test every possible interactions

m_χ

What else!

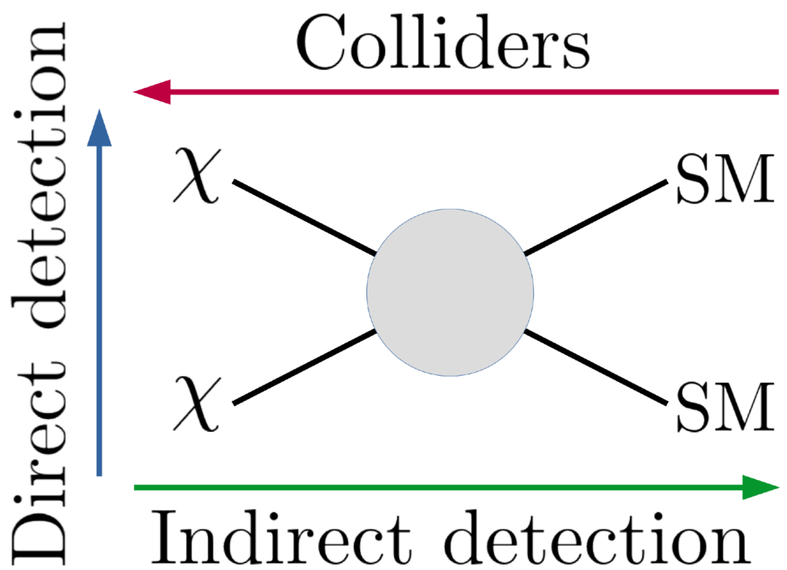

Test every possible interactions

- Discover DM
- Or set bounds

m_χ

What else!

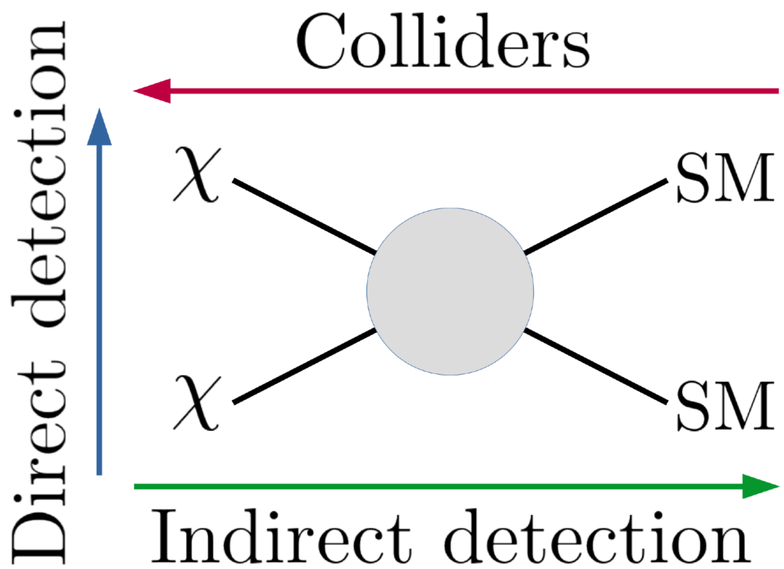

DM-electron scattering

↓

This talk

Test every possible interactions

- Discover DM
- Or set bounds

m_χ

Direct search: theory

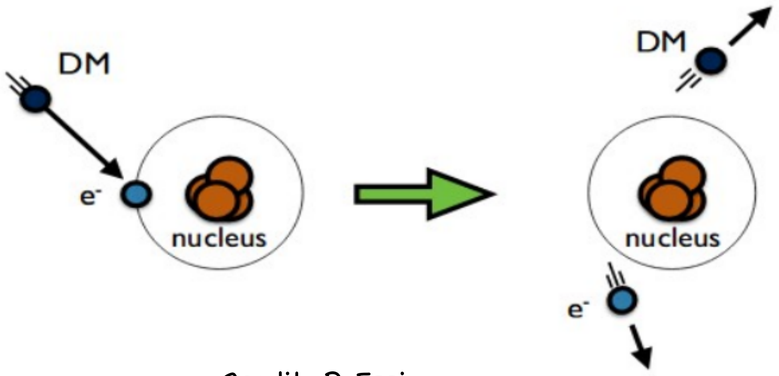

Credit: R Essig

arXiv: 1206.2644, 1108.5383, 1703.00910 ...

Direct search: theory

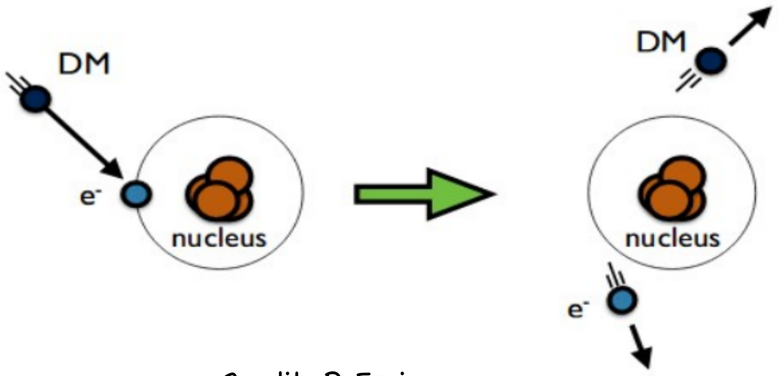

Credit: R Essig

$$\frac{dR_{\rm ion}}{d\,ln\,E_e} \propto N_T \frac{\bar{\sigma}_e}{8\mu_{\chi e}^2 m_\chi} \int q dq\, |f_{\rm ion}(E_e, q)|^2\, \rho_\chi\, \eta\left(v_{\rm min}(E_e, q)\right)$$

arXiv: 1206.2644, 1108.5383, 1703.00910 ...

Direct search: theory

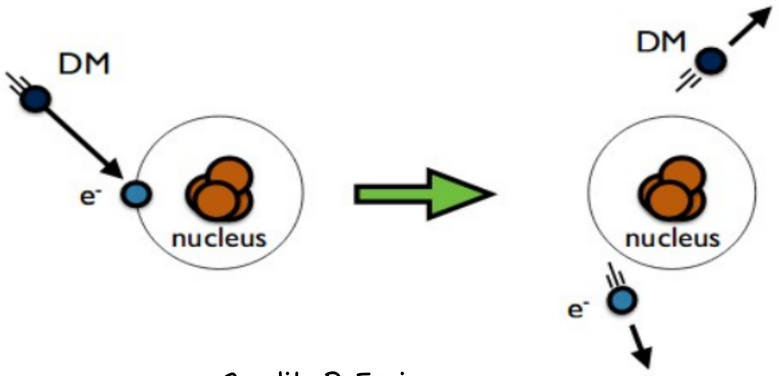

Credit: R Essig

target dependent

$$\frac{dR_{\rm ion}}{d\,ln\,E_e} \propto N_T \frac{\bar{\sigma}_e}{8\mu_{\chi e}^2 m_\chi} \int q dq\, |f_{\rm ion}(E_e, q)|^2\, \rho_\chi\, \eta\left(v_{\rm min}(E_e, q)\right)$$

arXiv: 1206.2644, 1108.5383, 1703.00910 ...

Direct search: theory

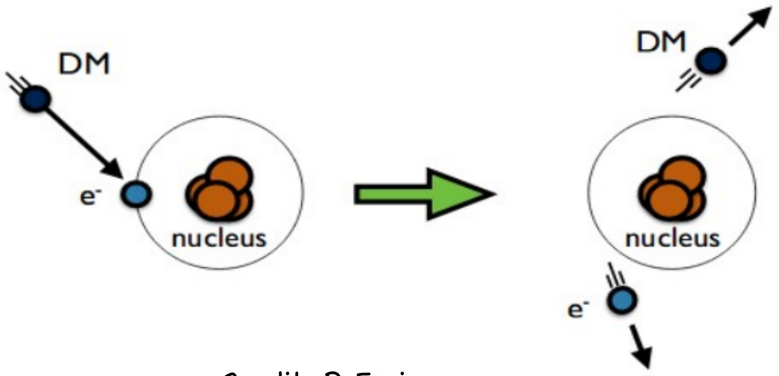

Credit: R Essig

target dependent

particle physics model

$$\frac{dR_{\rm ion}}{d\,ln\,E_e} \propto N_T \frac{\bar{\sigma}_e}{8\mu_{\chi e}^2 m_\chi} \int q dq\, |f_{\rm ion}(E_e, q)|^2\, \rho_\chi\, \eta\left(v_{\rm min}(E_e, q)\right)$$

arXiv: 1206.2644, 1108.5383, 1703.00910 ...

Direct search: theory

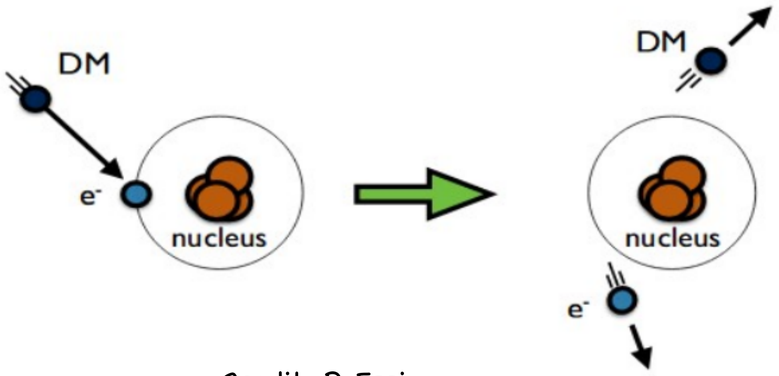

Credit: R Essig

target dependent

particle physics model

astrophysical input

$$\frac{dR_{\rm ion}}{d\,ln\,E_e} \propto N_T \frac{\bar{\sigma}_e}{8\mu_{\chi e}^2 m_\chi} \int q dq\, |f_{\rm ion}(E_e, q)|^2\, \rho_\chi\, \eta\left(v_{\rm min}(E_e, q)\right)$$

arXiv: 1206.2644, 1108.5383, 1703.00910 ...

Direct search: theory

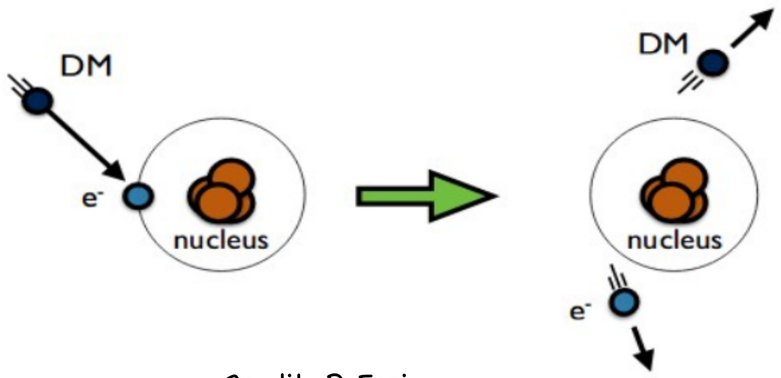

Credit: R Essig

target dependent

particle physics model

astrophysical input

$$\frac{dR_{\rm ion}}{d\,ln\,E_e} \propto N_T \frac{\bar{\sigma}_e}{8\mu_{\chi e}^2 m_\chi} \int q dq\, |f_{\rm ion}(E_e, q)|^2 \rho_\chi \eta\left(v_{\rm min}(E_e, q)\right)$$

$$\eta = \int_{v_{\rm min}}^{\infty} \frac{f(\vec{v} + \vec{v}_E)}{v} d^3v$$

Required minimum DM velocity

$$f(\vec{v}) \propto {\rm Exp}\left(-\frac{|\vec{v}|^2}{\sigma^2}\right) \Theta\left(v_{\rm esc} - |\vec{v}|\right)$$

Standard Halo Model (SHM)

arXiv: 1206.2644, 1108.5383, 1703.00910 ...

Direct search: experiment

Direct search: experiment

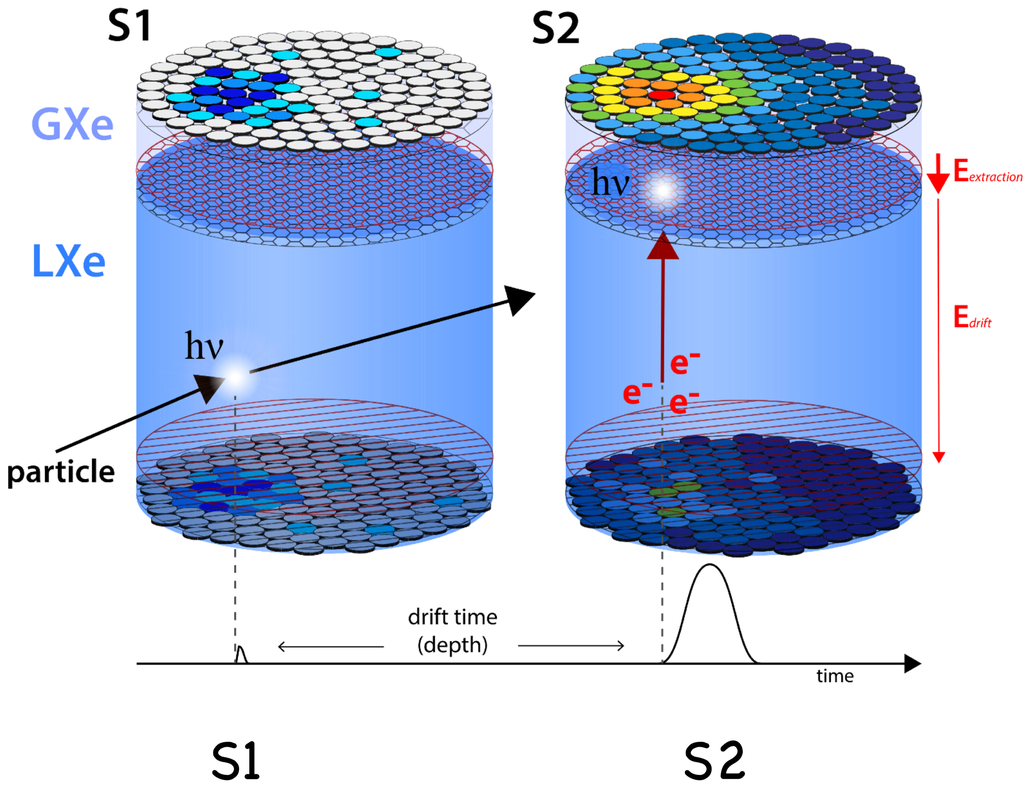

Direct search: experiment

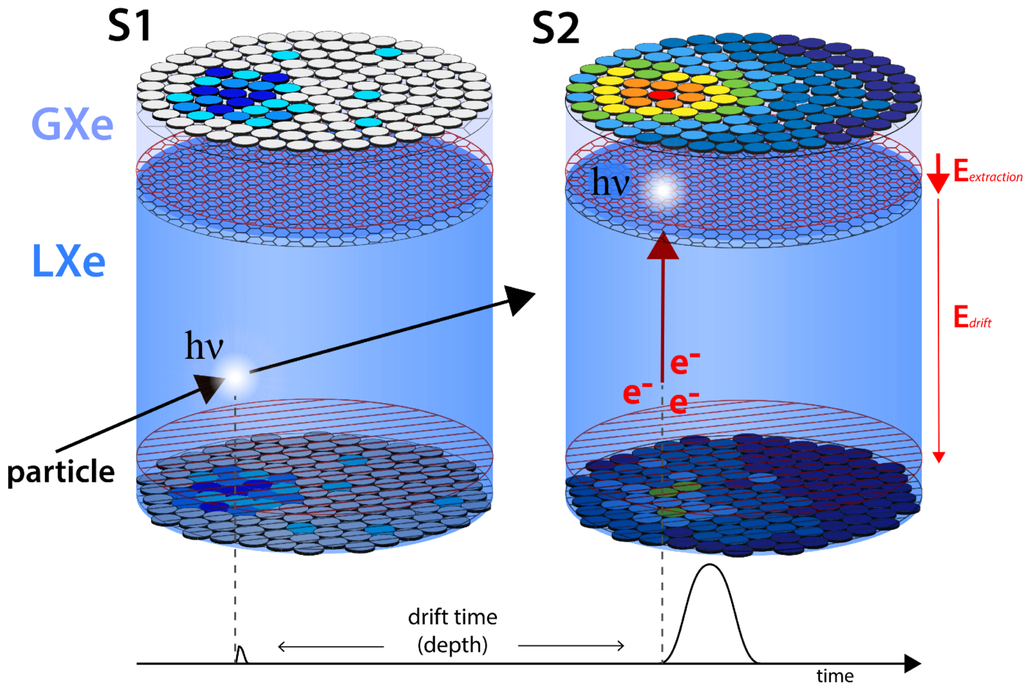

S1 << S2

Electron recoil signature

Direct search: experiment

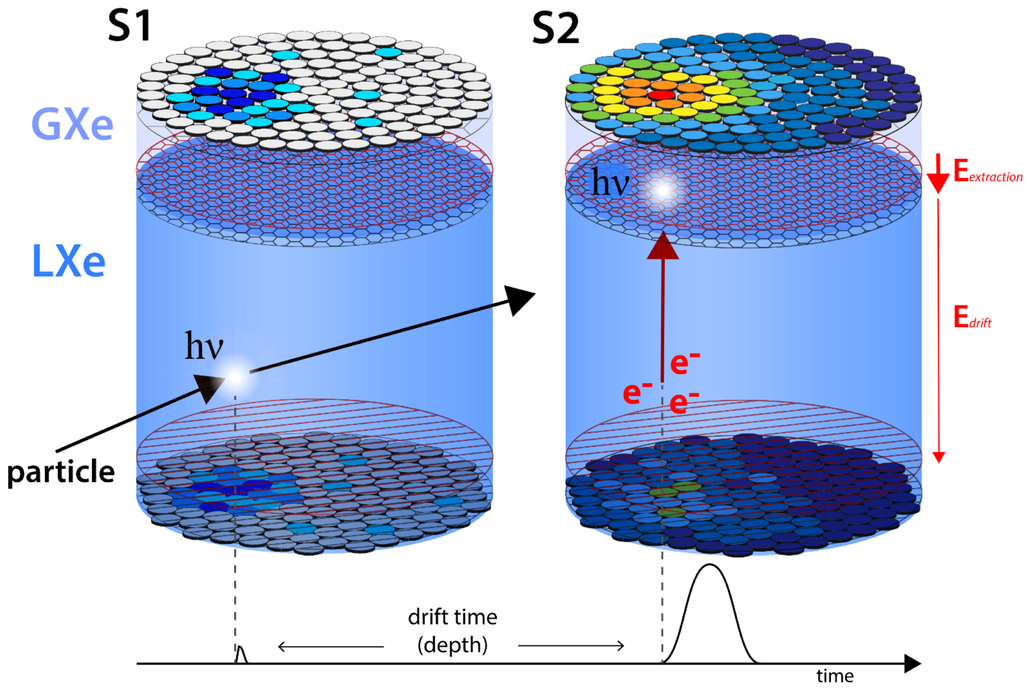

S1 << S2

Electron recoil signature

S2 only analysis

Direct search: experiment

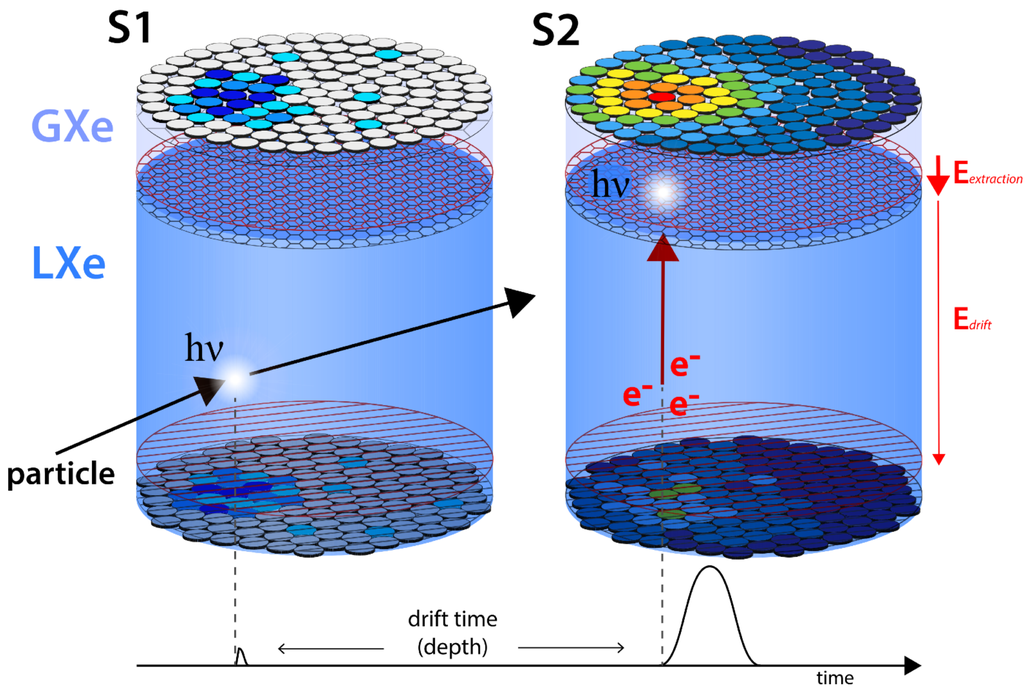

S1 << S2

Electron recoil signature

S2 only analysis

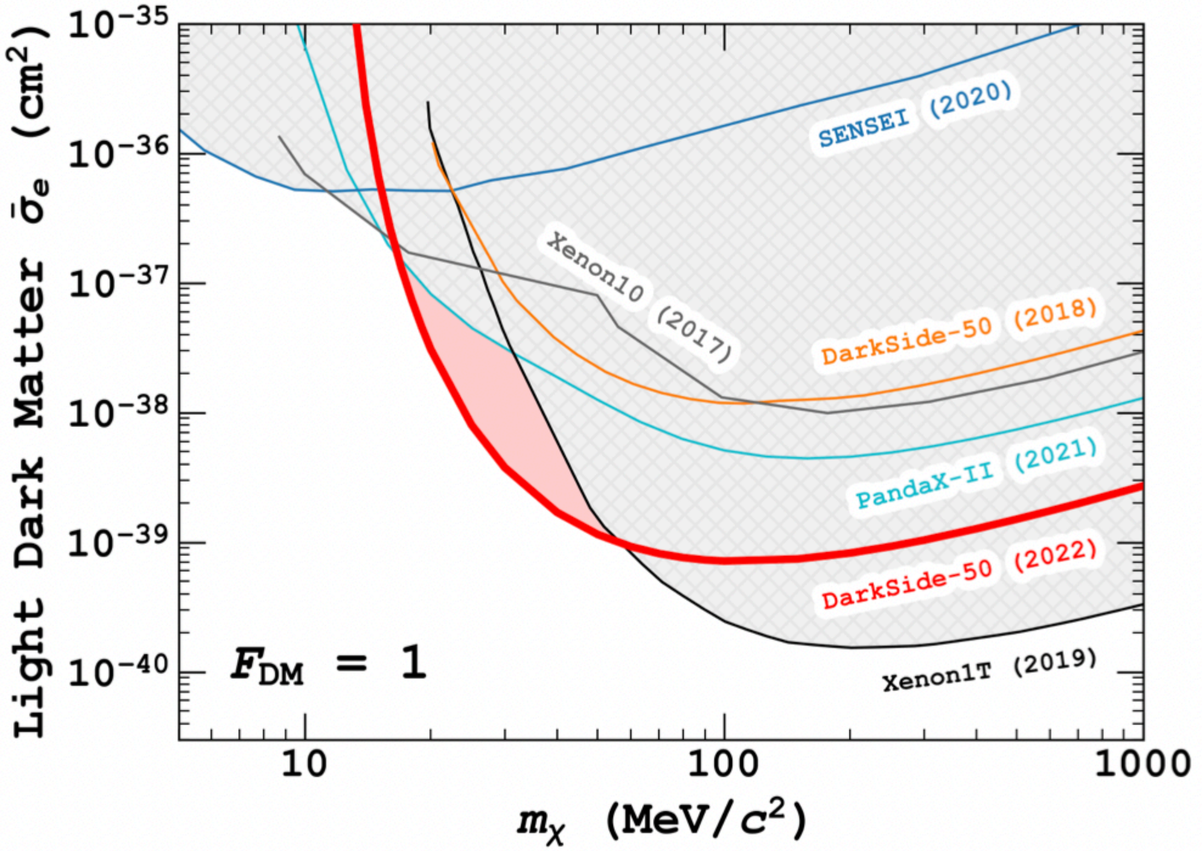

Direct search: experiment

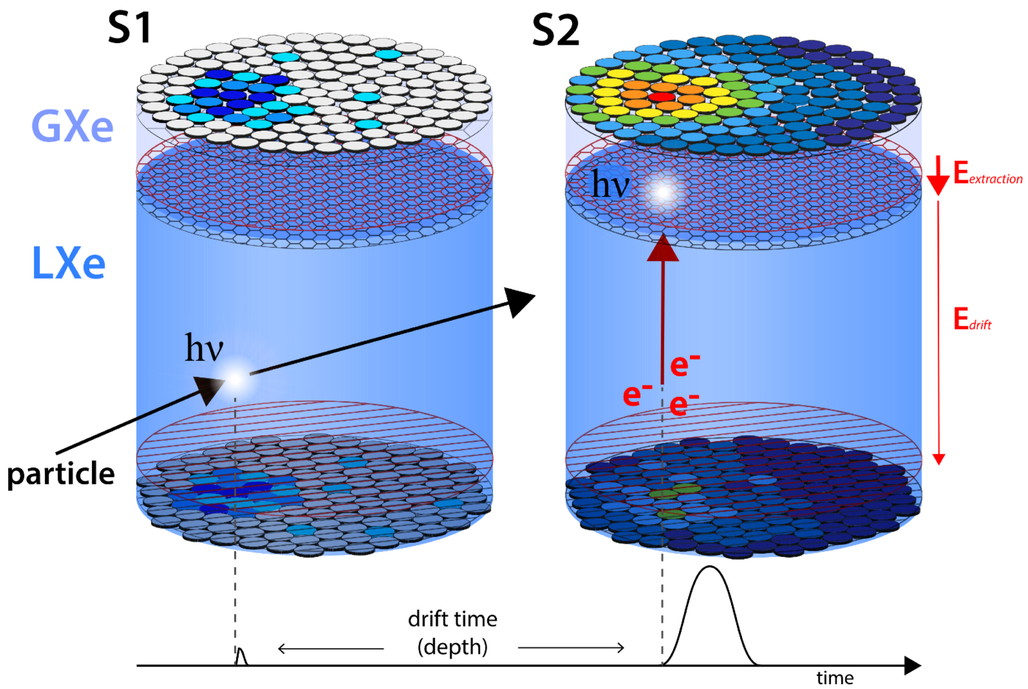

S1 << S2

Electron recoil signature

S2 only analysis

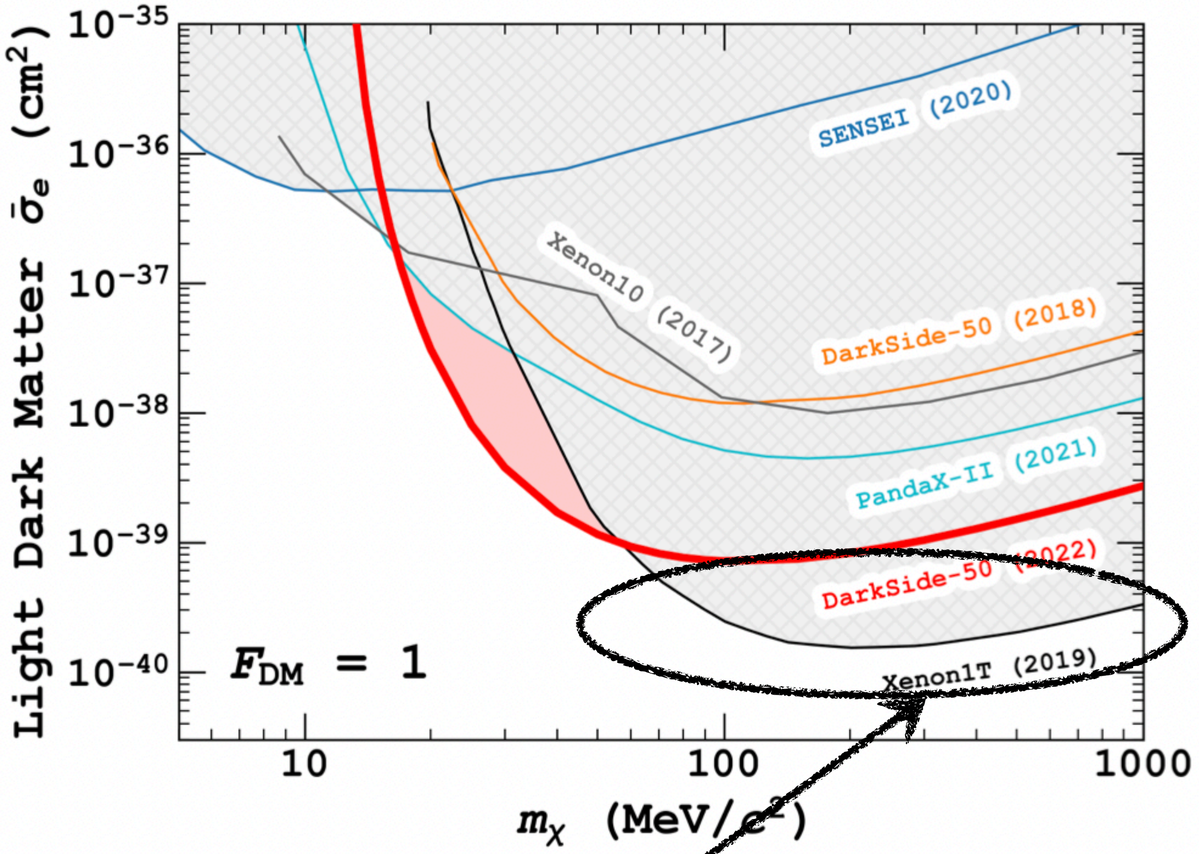

Strongest bound in large region of parameter space

Direct search: experiment

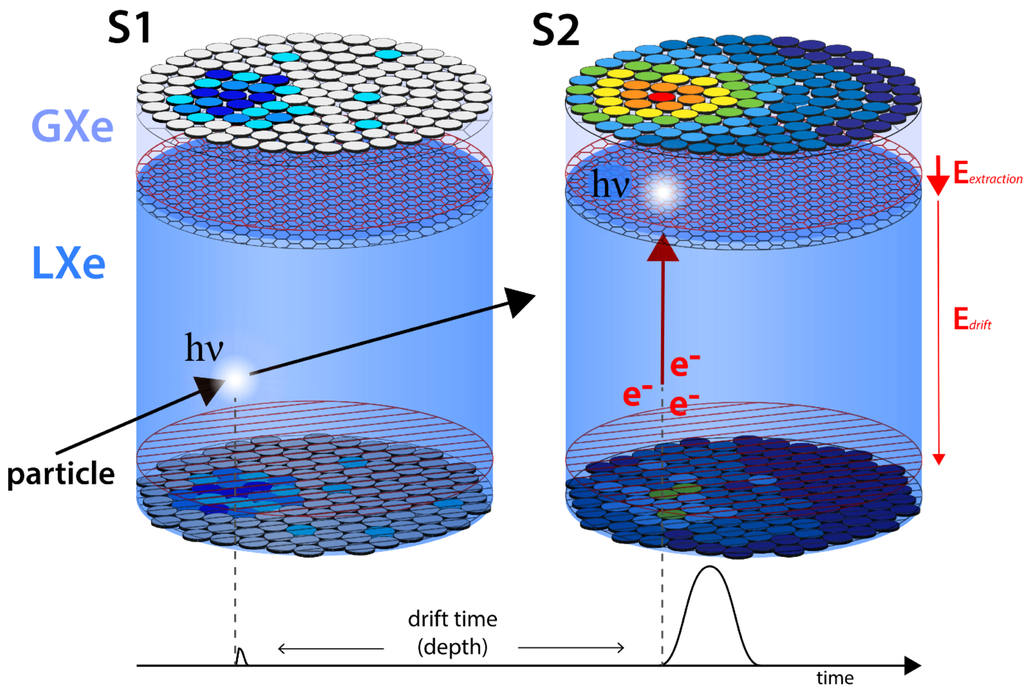

S1 << S2

Electron recoil signature

S2 only analysis

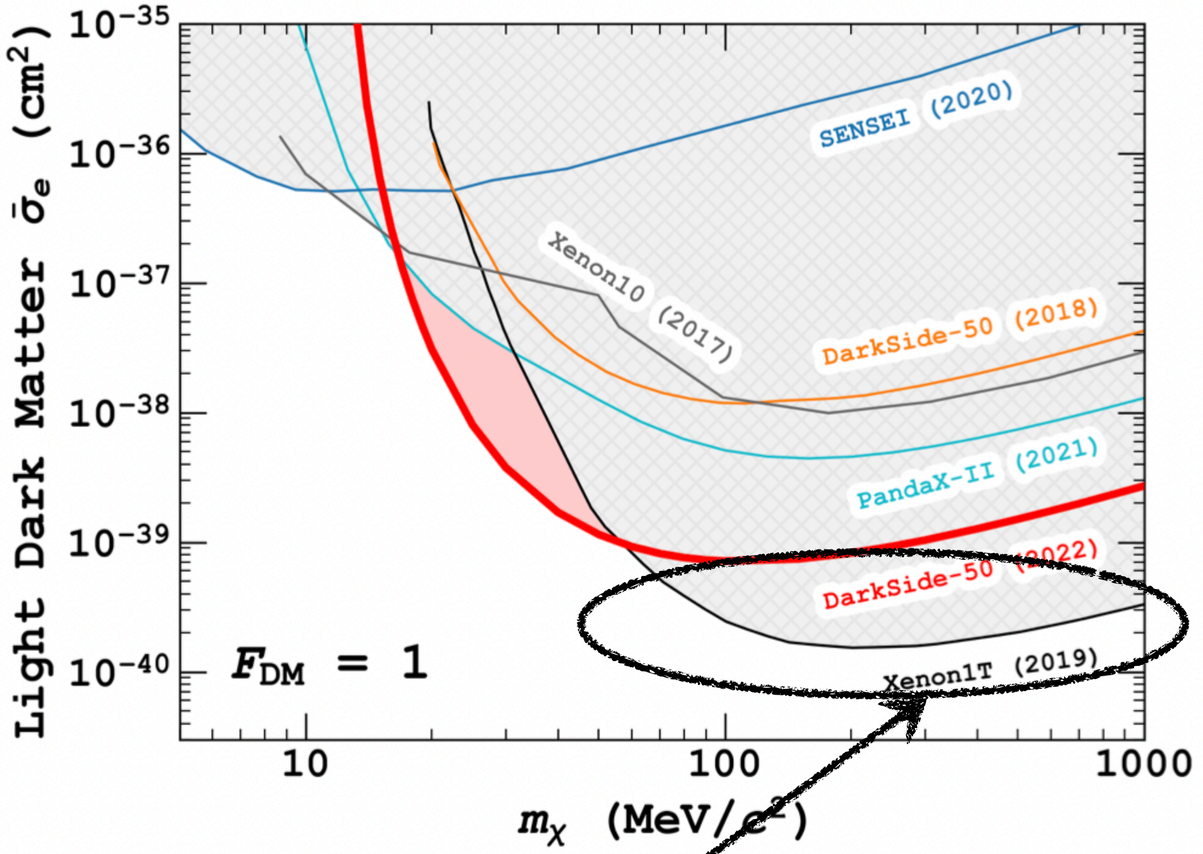

Strongest bound in large region of parameter space

Assuming SHM model →

Briefing: SHM

$$f(x, p, t)$$

Briefing: SHM

$$f(x, p, t)$$

Collision less Boltzmann Equation

$$\frac{\delta f}{\delta x} + \dot{x}\frac{\delta f}{\delta x} + \dot{p}\frac{\delta f}{\delta p} = 0$$

Briefing: SHM

$$f(x, p, t)$$

Collision less Boltzmann Equation

$$\frac{\delta f}{\delta x} + \dot{x}\frac{\delta f}{\delta x} + \dot{p}\frac{\delta f}{\delta p} = 0$$

Steady state

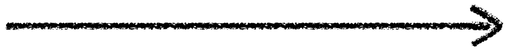

Isotropic velocities

Flat rotational curve

Briefing: SHM

$$f(x, p, t)$$

Collision less Boltzmann Equation

$$\frac{\delta f}{\delta x} + \dot{x}\frac{\delta f}{\delta x} + \dot{p}\frac{\delta f}{\delta p} = 0$$

Steady state

Isotropic velocities
Flat rotational curve

$$\rho \sim r^{-2}$$

$$f(\mathbf{v}) \sim e^{-|\mathbf{v}|^2/v_{\rm circ}^2}$$

Isothermal sphere

Briefing: SHM

$$f(x, p, t)$$

Collision less Boltzmann Equation

$$\frac{\delta f}{\delta x} + \dot{x}\frac{\delta f}{\delta x} + \dot{p}\frac{\delta f}{\delta p} = 0$$

Steady state

Isotropic velocities
Flat rotational curve

$$\rho \sim r^{-2}$$

$$f(\mathbf{v}) \sim e^{-|\mathbf{v}|^2/v_{\rm circ}^2}$$

Isothermal sphere

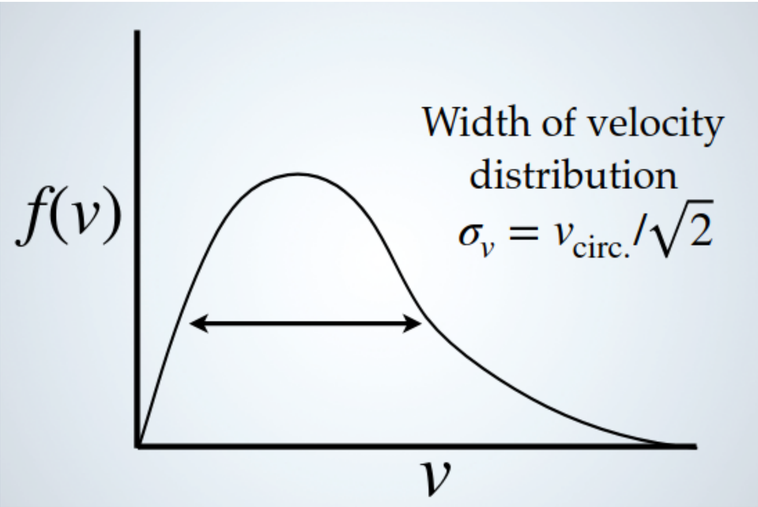

Cut off at escape velocity

Briefing: SHM

$$f(x, p, t)$$

Collision less Boltzmann Equation

$$\frac{\delta f}{\delta x} + \dot{x}\frac{\delta f}{\delta x} + \dot{p}\frac{\delta f}{\delta p} = 0$$

Steady state ?

Isotropic velocities

Flat rotational curve

$$\rho \sim r^{-2}$$

$$f(\mathbf{v}) \sim e^{-|\mathbf{v}|^2/v_{\rm circ}^2}$$

Isothermal sphere

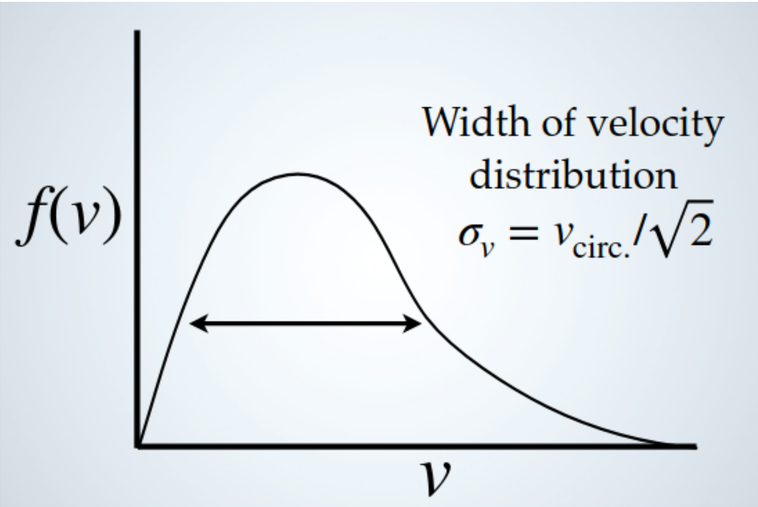

Cut off at escape velocity

Merger tree

Time

Now

Idea credit: M Lisanti

Merger tree

Time

Quiet merger

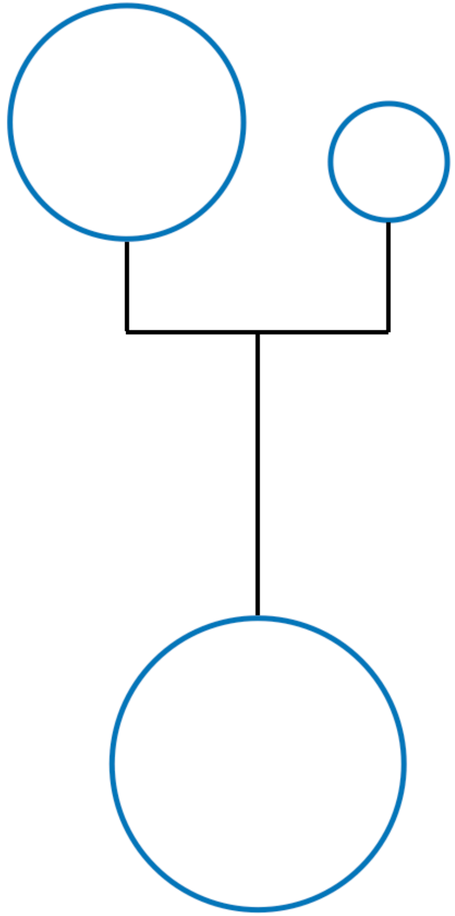

Now

Idea credit: M Lisanti

Merger tree

Time

Now

Quiet merger

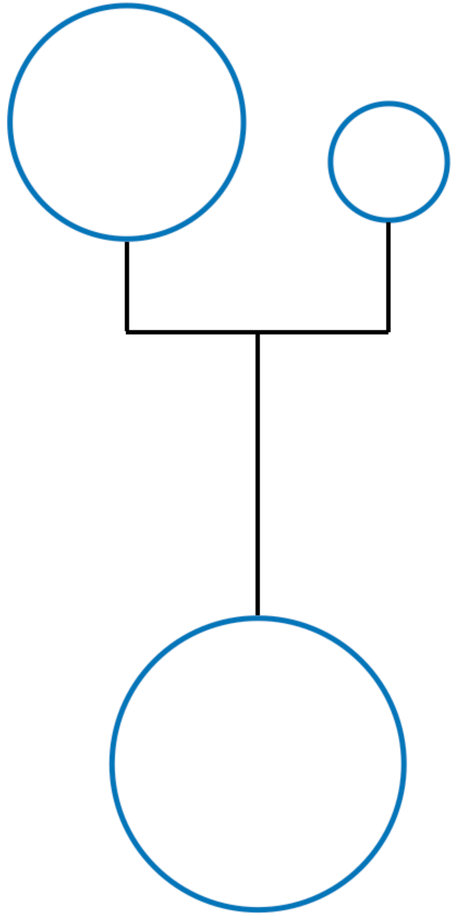

Steady state

Idea credit: M Lisanti

Merger tree

Time

Now

Quiet merger

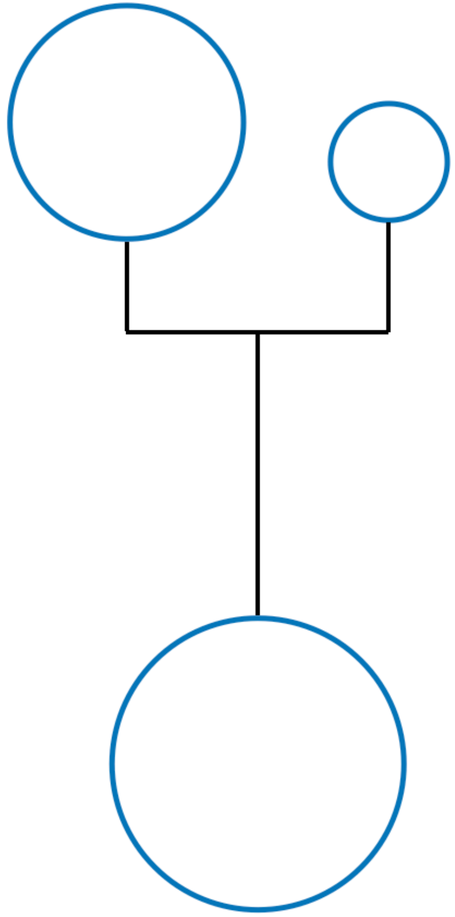

Steady state

Active merger

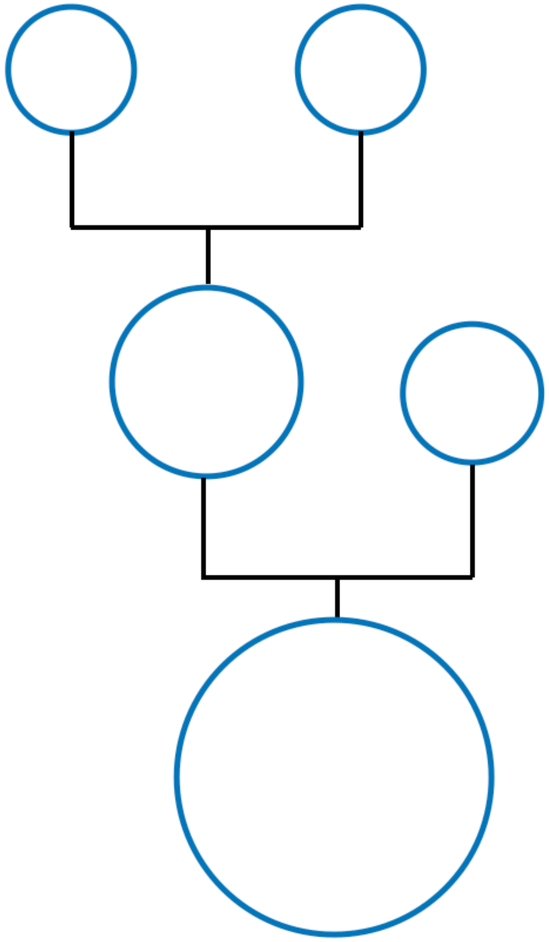

Idea credit: M Lisanti

Merger tree

Time

Now

Quiet merger

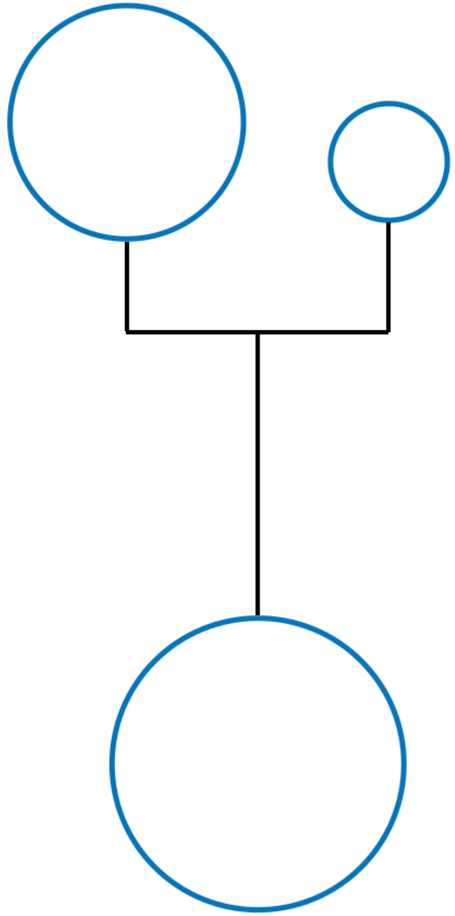

Steady state

Active merger

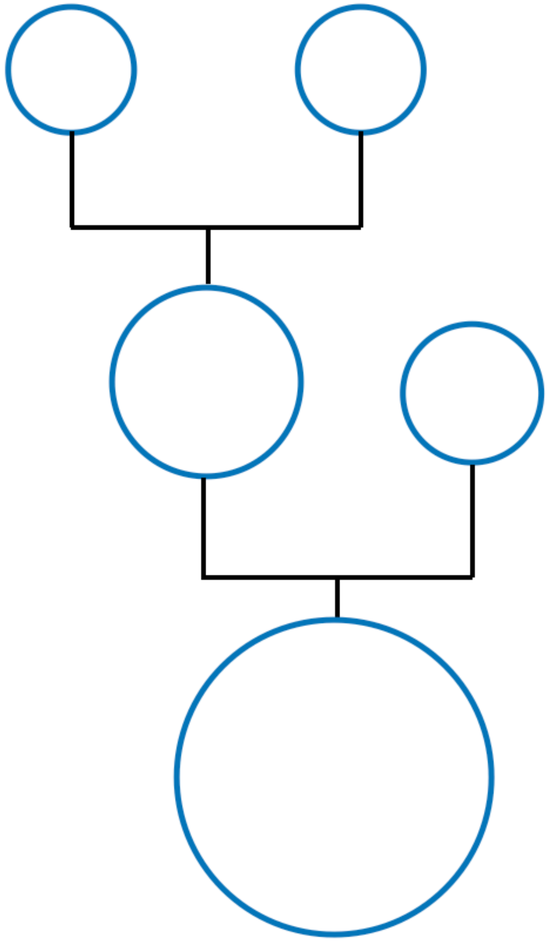

Steady state →

Idea credit: M Lisanti

Characterising merger tree ?

Characterising merger tree ?

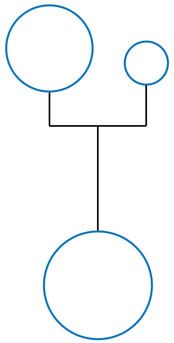

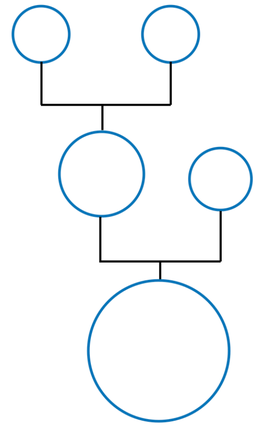

Characterising merger tree ?

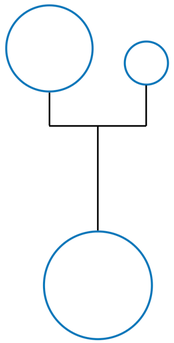

Options → Non-luminous component ?

Options → Luminous component (stars)

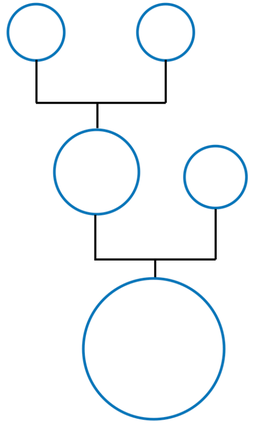

Characterising merger tree ?

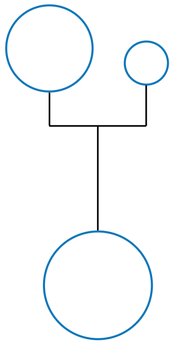

Options → Non-luminous component ?

Options → Luminous component (stars)

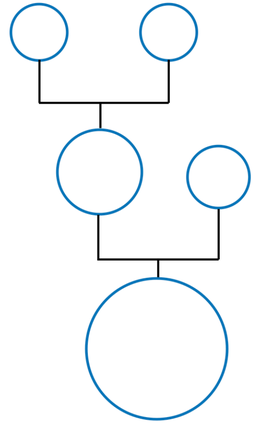

Characterising merger tree ?

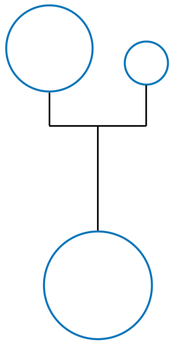

Options → Non-luminous component ?

Options → Luminous component (stars)

Missions: Gaia, LAMOST, etc.

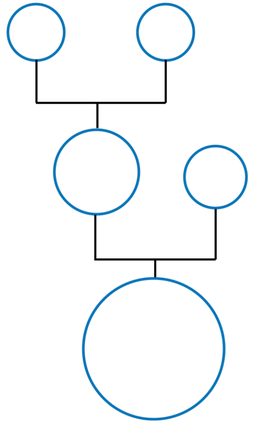

Characterising merger tree ?

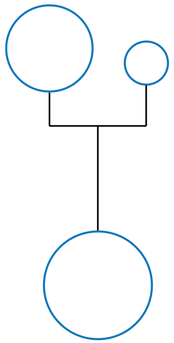

Options → Non-luminous component ?

Options → Luminous component (stars)

Missions: Gaia, LAMOST, etc.

Expectation

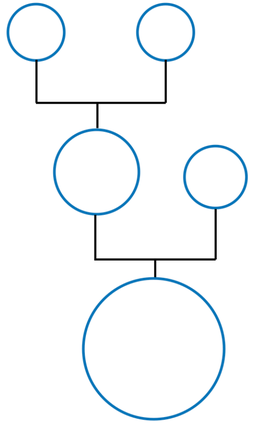

Characterising merger tree ?

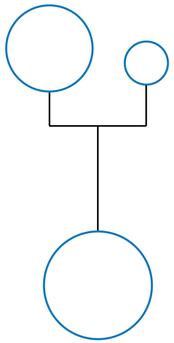

Options → Non-luminous component ?

→ Luminous component (stars)

↓

Missions: Gaia, LAMOST, etc.

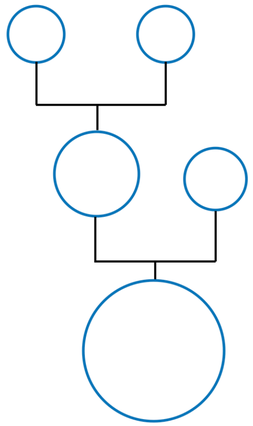

Expectation

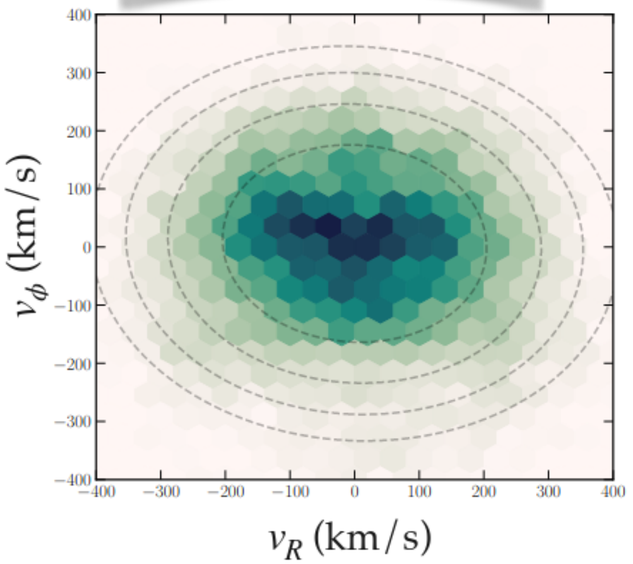

Characterising merger tree ?

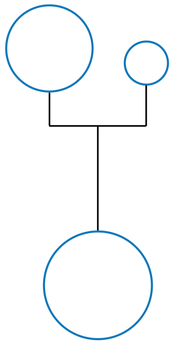

Options → Non-luminous component ?

Options → Luminous component (stars)

Missions: Gaia, LAMOST, etc.

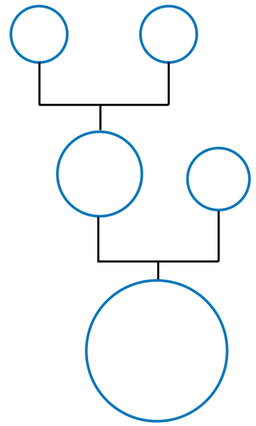

Expectation

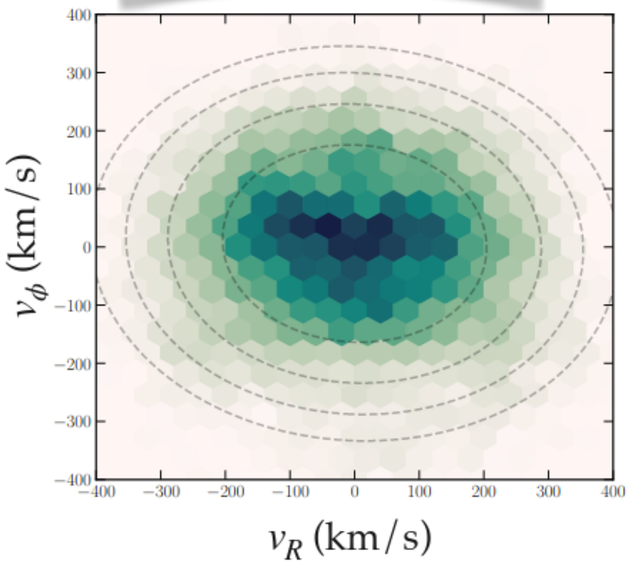

Roundish
Well mixed in phase space
Old merger

Image credit: C O'Hare

Characterising merger tree ?

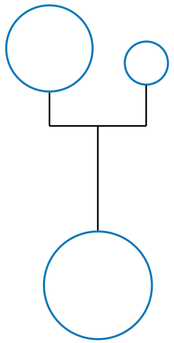

Options → Non-luminous component ?

Options → Luminous component (stars)

Missions: Gaia, LAMOST, etc.

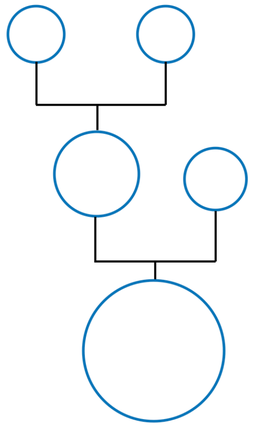

Expectation

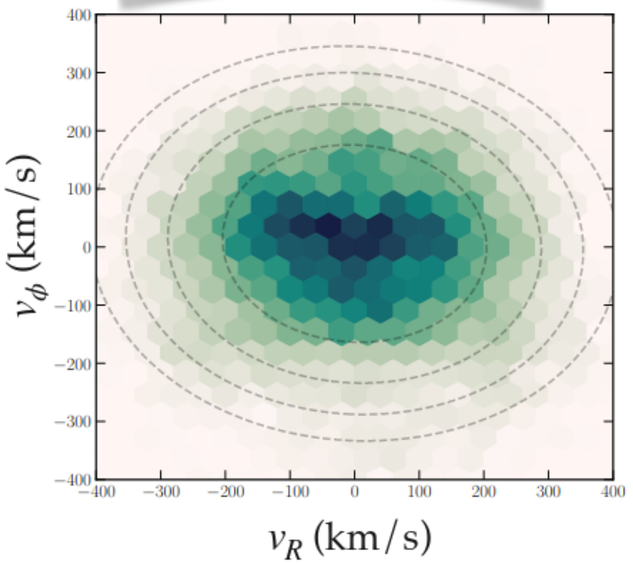

Reality

Roundish
Well mixed in phase space
Old merger

Image credit: C O'Hare

Characterising merger tree ?

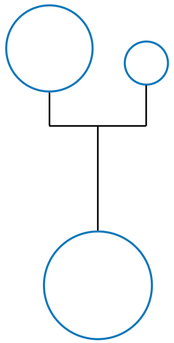

Options → Non-luminous component ?

→ Luminous component (stars)

↓

Missions: Gaia, LAMOST, etc.

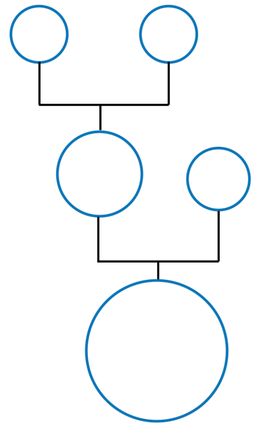

Expectation

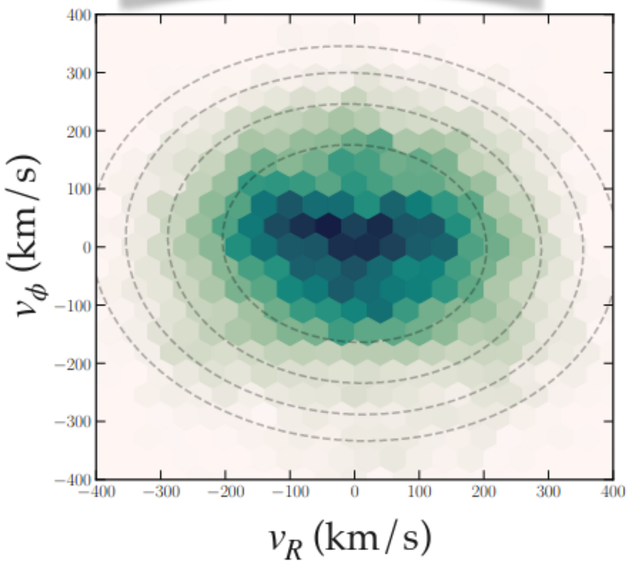

Roundish

Well mixed in phase space

Old merger

Reality

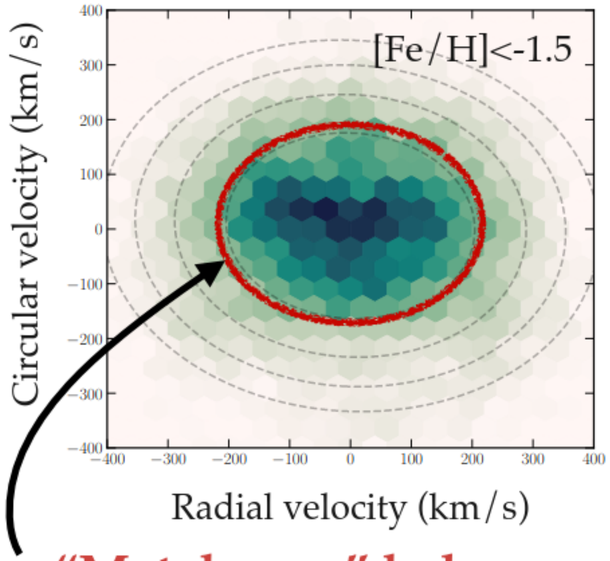

"Metal-poor" halo

Roundish

Well mixed in phase space

Old merger

Image credit: C O'Hare

Characterising merger tree ?

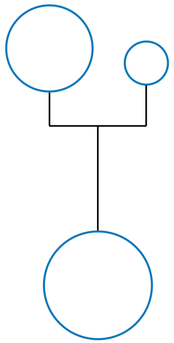

Options → Non-luminous component ?

→ Luminous component (stars)

↓

Missions: Gaia, LAMOST, etc.

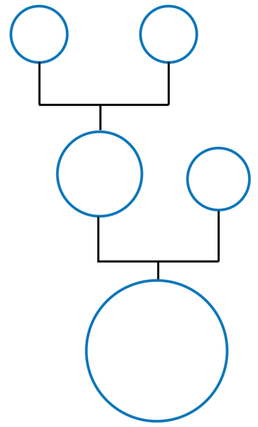

Expectation

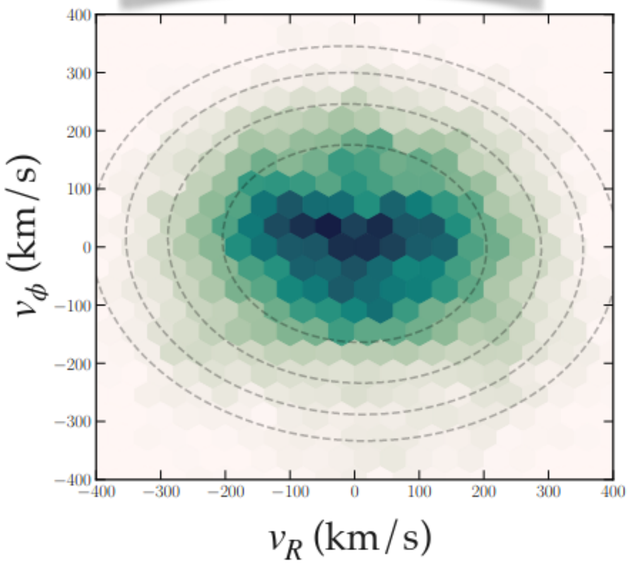

Roundish
Well mixed in phase space
Old merger

Reality

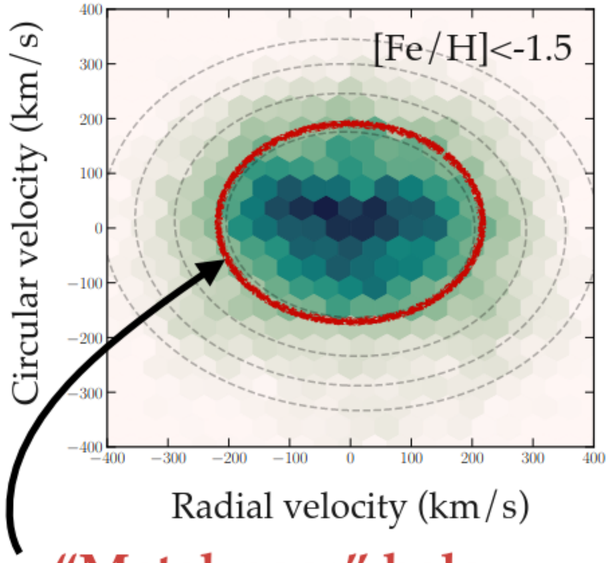

"Metal-poor" halo
Roundish
Well mixed in phase space
Old merger

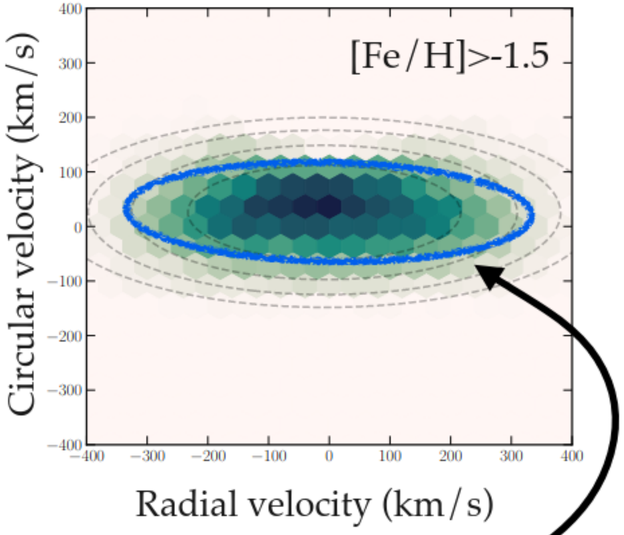

"Metal-rich" halo
Highly eccentric
Distinct feature in phase space
Rather recent merger

Image credit: C O'Hare

Characterising merger tree ?

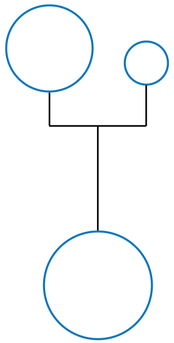

Options → Non-luminous component ?

→ Luminous component (stars)

↓

Missions: Gaia, LAMOST, etc.

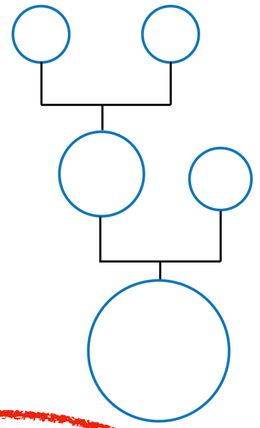

Expectation

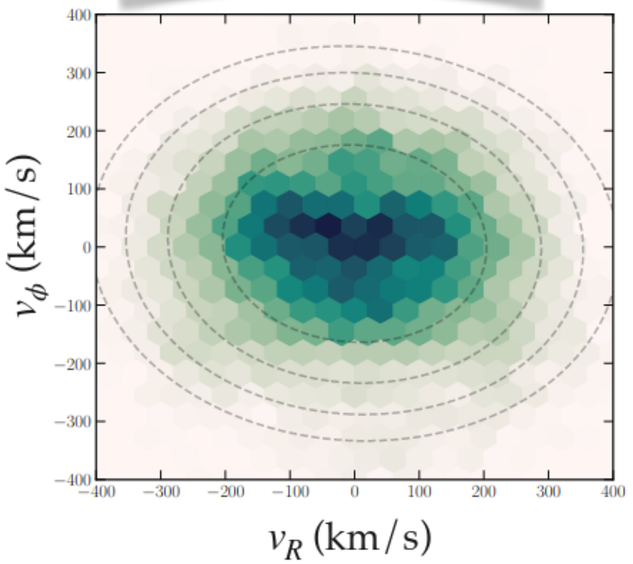

Roundish

Well mixed in phase space

Old merger

Reality

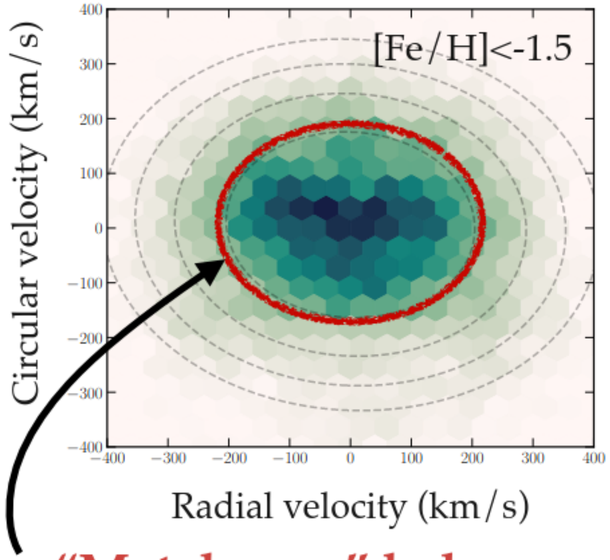

"Metal-poor" halo

Roundish

Well mixed in phase space

Old merger

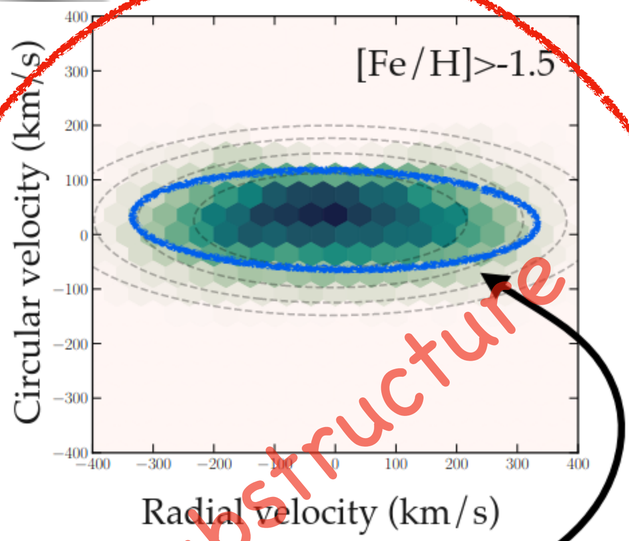

"Metal-rich" halo

Highly eccentric

Distinct feature in phase space

Rather recent merger

Substructure

Image credit: C O'Hare

Stellar/DM substructures?

[Submitted on 15 Jun 2018 (v1), last revised 31 Oct 2018 (this version, v2)]

The merger that led to the formation of the Milky Way's inner stellar halo and thick disk

Amina Helmi, Carine Babusiaux, Helmer H. Koppelman, Davide Massari, Jovan Veljanoski, Anthony G.A. Brown

The assembly process of our Galaxy can be retrieved using the motions and chemistry of individual stars. Chemo-dynamical studies of the nearby halo have long hinted at the presence of multiple components such as streams, clumps, duality and correlations between the stars'

the thick disk and the stellar halo. We demonstrate that the inner halo is dominated by debris from an object which at infall was slightly more massive than the Small Magellanic Cloud, and which we refer to as Gaia-Enceladus. The stars originating in Gaia-Enceladus cover nearly the full sky, their motions reveal the presence of streams and slightly retrograde and elongated trajectories.

to the dynamical heating of the precursor of the Galactic thick disk and therefore contributed to the formation of this component approximately 10 Gyr ago. These findings are in line with simulations of galaxy formation, which predict that the inner stellar halo should be dominated by debris from just a few massive progenitors.

[Submitted on 19 Apr 2018 (v1), last revised 2 Jul 2018 (this version, v3)]

The Shards of ω Centauri

G.C. Myeong (1), N.W. Evans (1), V. Belokurov (1), J.L. Sanders (1), S.E. Koposov (1,2) ((1) IoA, Cambridge, (2) CMU, Pittsburgh)

We use the SDSS–Gaia catalogue to search for substructure in the stellar halo. The sample comprises 63,132 halo stars with full phase

secondary check. This is validated against smooth models and numerical constructed stellar halos from the Aquarius simulations. We identify 21 substructures in the SDSS-Gaia catalogue, including 7 high significance, high energy and retrograde ones.

bring ω~Centauri to its current location in action -- energy space. Our proposal can be tested by high resolution spectroscopy of the candidates to look for the unusual abundance patterns possessed by ω~Centauri stars.

[Submitted on 15 Jun 2020]

Evidence from the H3 Survey that the Stellar Halo is Entirely Comprised of Substructure

Rohan P. Naidu, Charlie Conroy, Ana Bonaca, Benjamin D. Johnson, Yuan-Sen Ting, Nelson Caldwell, Dennis Zaritsky, Phillip A. Cargile

In the ΛCDM paradigm the Galactic stellar halo is predicted to harbor the accreted debris of smaller systems. To identify these systems, the

5684 giants at $|b| > 40^\circ$ and $|Z| > 2$ kpc. We identify known structures including the high-α disk, the in-situ halo (disk stars heated to eccentric orbits), Sagittarius (Sgr), *Gaia*-Sausage-Enceladus (GSE), the Helmi Streams, Sequoia, and Thamnos. Additionally, we identify the following new structures: (i) Aleph

80% of the halo is built by two massive ($M_\star \sim 10^8 - 10^9 M_\odot$) accreted dwarfs: GSE ([Fe/H]$= -1.2$) within 25 kpc, and Sgr ([Fe/H]$= -1.0$) beyond 25 kpc. This explains the relatively high overall metallicity of the halo ([Fe/H]≈ -1.2). We attribute $\gtrsim$95% of the sample to one of the listed structures, pointing to a halo built entirely from accreted dwarfs and heating of the disk.

[Submitted on 16 Oct 2019]

Dynamical Relics of the Ancient Galactic Halo

Zhen Yuan (1), G.C. Myeong (2,3), Timothy C. Beers (4), N. Wyn Evans (3), Young Sun Lee (5), Projjwal Banerjee (6), Dmitrii Gudin (4), Kohei Hattori (7), Haining Li (8), Tadafumi Matsuno (9), Vinicius M. Placco (4), M. C. Smith (1), Devin D. Whitten (4), Gang Zhao (8) ((1) SAO, Shanghai, (2) CfA, Harvard, (3) IoA, Cambridge, (4) Notre Dame, (5) Chungnam Univ, Daejeon, (6) Indian Institute of Technology, Palakkad, (7) CMU, Pittsburgh (8) NAO, Beijing, (9) NAOJ, Tokyo)

space of orbital energy and angular momentum. We identify 57 dynamically tagged groups, which we label DTG-1 to DTG-57. Most of them belong to existing substructures in the nearby halo, such as the *Gaia* Sausage or Sequoia. The stream identified by Helmi et al. is recovered, but the two disjoint portions of

and look for associations with chemically peculiar stars. The highly eccentric *Gaia* Sausage groups contain representatives both of debris from the satellite itself (which is α-poor) and the Splashed Disk, sent up into eccentric halo orbits from the encounter (and is α-rich). The new prograde substructures also appear to be associated with the Splashed Disk. The DTGs belonging to the *Gaia* Sausage host two relatively metal-rich r-II stars and six CEMP stars in different sub-classes, consistent with the idea that the *Gaia* Sausage progenitor is a massive dwarf galaxy. Rg5 is dynamically associated with two highly r-process-enhanced stars with [Fe/H] ~ -3. This finding indicates that its progenitor might be an ultra-faint dwarf galaxy that has experienced r-process enrichment from neutron star mergers.

+ many more

Stellar/DM substructures?

arXiv > astro-ph > arXiv:1806.06038

Astrophysics > Astrophysics of Galaxies

[Submitted on 15 Jun 2018 (v1), last revised 31 Oct 2018 (this version, v2)]

The merger that led to the formation of the Milky Way's inner stellar halo and thick disk

Amina Helmi, Carine Babusiaux, Helmer H. Koppelman, Davide Massari, Jovan Veljanoski, Anthony G.A. Brown

The assembly process of our Galaxy can be retrieved using the motions and chemistry of individual stars. Chemo-dynamical studies of the nearby halo have long hinted at the presence of multiple components such as streams, clumps, duality and correlations between the stars'

the thick disk and the stellar halo. We demonstrate that the inner halo is dominated by debris from an object which at infall was slightly more massive than the Small Magellanic Cloud, and which we refer to as Gaia-Enceladus. The stars originating in Gaia-Enceladus cover nearly the full sky, their motions reveal the presence of streams and slightly retrograde and elongated trajectories.

to the dynamical heating of the precursor of the Galactic thick disk and therefore contributed to the formation of this component approximately 10 Gyr ago. These findings are in line with simulations of galaxy formation, which predict that the inner stellar halo should be dominated by debris from just a few massive progenitors.

arXiv > astro-ph > arXiv:1804.07050

Astrophysics > Astrophysics of Galaxies

[Submitted on 19 Apr 2018 (v1), last revised 2 Jul 2018 (this version, v3)]

The Shards of ω Centauri

G.C. Myeong (1), N.W. Evans (1), V. Belokurov (1), J.L. Sanders (1), S.E. Koposov (1,2) ((1) IoA, Cambridge, (2) CMU, Pittsburgh)

secondary check. This is validated against smooth models and numerical constructed stellar halos from the Aquarius simulations. We identify 21 substructures in the SDSS-Gaia catalogue, including 7 high significance, high energy and retrograde ones.

bring ω~Centauri to its current location in action -- energy space. Our proposal can be tested by high resolution spectroscopy of the candidates to look for the unusual abundance patterns possessed by ω~Centauri stars.

arXiv > astro-ph > arXiv:2006.08625

Astrophysics > Astrophysics of Galaxies

[Submitted on 15 Jun 2020]

Evidence from the H3 Survey that the Stellar Halo is Entirely Comprised of Substructure

Rohan P. Naidu, Charlie Conroy, Ana Bonaca, Benjamin D. Johnson, Yuan-Sen Ting, Nelson Caldwell, Dennis Zaritsky, Phillip A. Cargile

In the ΛCDM paradigm the Galactic stellar halo is predicted to harbor the accreted debris of smaller systems. To identify these systems, the

5684 giants at $|b| > 40^\circ$ and $|Z| > 2$ kpc. We identify known structures including the high-α disk, the in-situ halo (disk stars heated to eccentric orbits), Sagittarius (Sgr), *Gaia*-Sausage-Enceladus (GSE), the Helmi Streams, Sequoia, and Thamnos. Additionally, we identify the following new structures: (i) Aleph

80% of the halo is built by two massive ($M_\star \sim 10^8 - 10^9 M_\odot$) accreted dwarfs: GSE ([Fe/H]$= -1.2$) within 25 kpc, and Sgr ([Fe/H]$= -1.0$) beyond 25 kpc. This explains the relatively high overall metallicity of the halo ([Fe/H]≈ -1.2). We attribute $\gtrsim$95% of the sample to one of the listed structures, pointing to a halo built entirely from accreted dwarfs and heating of the disk.

arXiv > astro-ph > arXiv:1910.07538

Astrophysics > Astrophysics of Galaxies

[Submitted on 16 Oct 2019]

Dynamical Relics of the Ancient Galactic Halo

Zhen Yuan (1), G.C. Myeong (2,3), Timothy C. Beers (4), N. Wyn Evans (3), Young Sun Lee (5), Projjwal Banerjee (6), Dmitrii Gudin (4), Kohei Hattori (7), Haining Li (8), Tadafumi Matsuno (9), Vinicius M. Placco (4), M. C. Smith (1), Devin D. Whitten (4), Gang Zhao (8) ((1) SAO, Shanghai, (2) CfA, Harvard, (3) IoA, Cambridge, (4) Notre Dame, (5) Chungnam Univ, Daejeon, (6) Indian Institute of Technology, Palakkad, (7) CMU, Pittsburgh (8) NAO, Beijing, (9) NAOJ, Tokyo)

space of orbital energy and angular momentum. We identify 57 dynamically tagged groups, which we label DTG-1 to DTG-57. Most of them belong to existing substructures in the nearby halo, such as the *Gaia* Sausage or Sequoia. The stream identified by Helmi et al. is recovered, but the two disjoint portions of

and look for associations with chemically peculiar stars. The highly eccentric *Gaia* Sausage groups contain representatives both of debris from the satellite itself (which is α-poor) and the Splashed Disk, sent up into eccentric halo orbits from the encounter (and is α-rich). The new prograde substructures also appear to be associated with the Splashed Disk. The DTGs belonging to the *Gaia* Sausage host two relatively metal-rich r-II stars and six CEMP stars in different sub-classes, consistent with the idea that the *Gaia* Sausage progenitor is a massive dwarf galaxy. Rg5 is dynamically associated with two highly r-process-enhanced stars with [Fe/H] ~ -3. This finding indicates that its progenitor might be an ultra-faint dwarf galaxy that has experienced r-process enrichment from neutron star mergers.

⊖ We assume DM and stars follows same velocity distribution

+ many more

DM substructures + SHM

Substructure	Mean velocity (km/s)			Velocity dispersion (km/s)		
	μ_R	μ_ϕ	μ_z	σ_R	σ_ϕ	σ_z
HelmiDTG1	4.5	197.2	244.3	146.0	62.6	42.4
HelmiDTG3	26.2	157.1	-241.3	78.9	28.8	27.2
PolarDTG11	-47.9	21.8	229.2	75.4	19.2	21.5
PgDTG2	221.2	155.7	139.7	26.2	33.8	52.3
Sausage	2.1	-0.3	-8.7	136.6	35.0	72.3
RgDTG28	-4.0	-106.1	-143.2	115.8	29.3	30.3
Sequoia	-36.9	-273.9	-87.0	138.2	36.7	65.0
SHM	0.	0.	0.	155.6	155.6	155.6

$$\frac{dR_{\rm ion}}{d\,ln\,E_e} \propto N_T \frac{\bar{\sigma}_e}{8\mu_{\chi e}^2 m_\chi} \int q dq\, |f_{\rm ion}(E_e, q)|^2\, \rho_\chi\, \eta\left(v_{\rm min}(E_e, q)\right)$$

$$\eta(v_{\rm min}) = \int_{v_{\rm min}}^{\infty} \frac{1}{v} \left[(1-\delta) f_{\rm lab}^{\rm SHM}(\mathbf{v}) + \delta f_{\rm lab}^{\zeta_i}(\mathbf{v})\right] d^3v$$

DM substructures + SHM

Substructure	Mean velocity (km/s)			Velocity dispersion (km/s)		
	μ_R	μ_ϕ	μ_z	σ_R	σ_ϕ	σ_z
HelmiDTG1	4.5	197.2	244.3	146.0	62.6	42.4
HelmiDTG3	26.2	157.1	-241.3	78.9	28.8	27.2
PolarDTG11	-47.9	21.8	229.2	75.4	19.2	21.5
PgDTG2	221.2	155.7	139.7	26.2	33.8	52.3
Sausage	2.1	-0.3	-8.7	136.6	35.0	72.3
RgDTG28	-4.0	-106.1	-143.2	115.8	29.3	30.3
Sequoia	-36.9	-273.9	-87.0	138.2	36.7	65.0
SHM	0.	0.	0.	155.6	155.6	155.6

$$\frac{dR_{\rm ion}}{d\,ln\,E_e} \propto N_T \frac{\bar{\sigma}_e}{8\mu_{\chi e}^2 m_\chi} \int qdq\,|f_{\rm ion}(E_e,q)|^2\,\rho_\chi\,\eta\left(v_{\rm min}(E_e,q)\right)$$

$$\eta(v_{\rm min}) = \int_{v_{\rm min}}^{\infty} \frac{1}{v}\left[(1-\delta) f_{\rm lab}^{\rm SHM}(\mathbf{v}) + \delta f_{\rm lab}^{\zeta_i}(\mathbf{v})\right] d^3v$$

Substructure fraction

DM substructures + SHM

Substructure	Mean velocity (km/s)			Velocity dispersion (km/s)		
	μ_R	μ_ϕ	μ_z	σ_R	σ_ϕ	σ_z
HelmiDTG1	4.5	197.2	244.3	146.0	62.6	42.4
HelmiDTG3	26.2	157.1	-241.3	78.9	28.8	27.2
PolarDTG11	-47.9	21.8	229.2	75.4	19.2	21.5
PgDTG2	221.2	155.7	139.7	26.2	33.8	52.3
Sausage	2.1	-0.3	-8.7	136.6	35.0	72.3
RgDTG28	-4.0	-106.1	-143.2	115.8	29.3	30.3
Sequoia	-36.9	-273.9	-87.0	138.2	36.7	65.0
SHM	0.	0.	0.	155.6	155.6	155.6

$$\frac{dR_{\rm ion}}{d\,ln\,E_e} \propto N_T \frac{\bar{\sigma}_e}{8\mu_{\chi e}^2 m_\chi} \int qdq\,|f_{\rm ion}(E_e,q)|^2\,\rho_\chi\,\eta\left(v_{\rm min}(E_e,q)\right)$$

$$\eta(v_{\rm min}) = \int_{v_{\rm min}}^{\infty} \frac{1}{v}\left[(1-\delta) f_{\rm lab}^{\rm SHM}(\mathbf{v}) + \delta f_{\rm lab}^{\zeta_i}(\mathbf{v})\right] d^3v$$

Substructure fraction

Astrophysics > Astrophysics of Galaxies

[Submitted on 7 Jan 2022 (v1), last revised 28 Apr 2022 (this version, v4)]

Substructure in the stellar halo near the Sun. II. Characterisation of independent structures

Tomás Ruiz-Lara, Tadafumi Matsuno, S. Sofie Lövdal, Amina Helmi, Emma Dodd, Helmer H. Koppelman

In Lövdal et al, we presented a data-driven method for clustering in Integrals of Motion space and applied it to a large sample of nearby halo stars with 6D phase-space information. We identified a large number of clusters, many of which could tentatively be merged into larger groups. Our goal is to establish the reality of the clusters through a combined study of their stellar populations to gain more insights into the accretion history of the Milky Way. We develop a procedure that quantifies the similarity of clusters based on KS tests using their metallicity distribution functions, and an isochrone fitting method to determine their average age, which is also used to compare the distribution of stars in the Colour-Absolute magnitude diagram. This allows us to group clusters into substructures, and to compare substructures with one another. The clusters identified are merged into 12 extended substructures, while 8 small clusters remain as such. The large substructures include the previously known Gaia-Enceladus, Helmi streams, Sequoia, and Thamnos 1 and 2. We identify overdensities associated with the hot thick disc and hosting a metal-poor population. Especially notable is our largest substructure which,

confirming our dissection of the nearby halo. At least 20\% of the halo near the Sun is associated to substructures. When comparing their

older.

DM substructures + SHM

Substructure	Mean velocity (km/s)			Velocity dispersion (km/s)		
	μ_R	μ_ϕ	μ_z	σ_R	σ_ϕ	σ_z
HelmiDTG1	4.5	197.2	244.3	146.0	62.6	42.4
HelmiDTG3	26.2	157.1	-241.3	78.9	28.8	27.2
PolarDTG11	-47.9	21.8	229.2	75.4	19.2	21.5
PgDTG2	221.2	155.7	139.7	26.2	33.8	52.3
Sausage	2.1	-0.3	-8.7	136.6	35.0	72.3
RgDTG28	-4.0	-106.1	-143.2	115.8	29.3	30.3
Sequoia	-36.9	-273.9	-87.0	138.2	36.7	65.0
SHM	0.	0.	0.	155.6	155.6	155.6

$$\frac{dR_{\rm ion}}{d\,ln\,E_e} \propto N_T \frac{\bar{\sigma}_e}{8\mu_{\chi e}^2 m_\chi} \int qdq\,|f_{\rm ion}(E_e,q)|^2\,\rho_\chi\,\eta\left(v_{\rm min}(E_e,q)\right)$$

$$\eta(v_{\rm min}) = \int_{v_{\rm min}}^{\infty} \frac{1}{v}\left[(1-\delta) f_{\rm lab}^{\rm SHM}(\mathbf{v}) + \delta f_{\rm lab}^{\zeta_i}(\mathbf{v})\right] d^3v$$

Substructure fraction

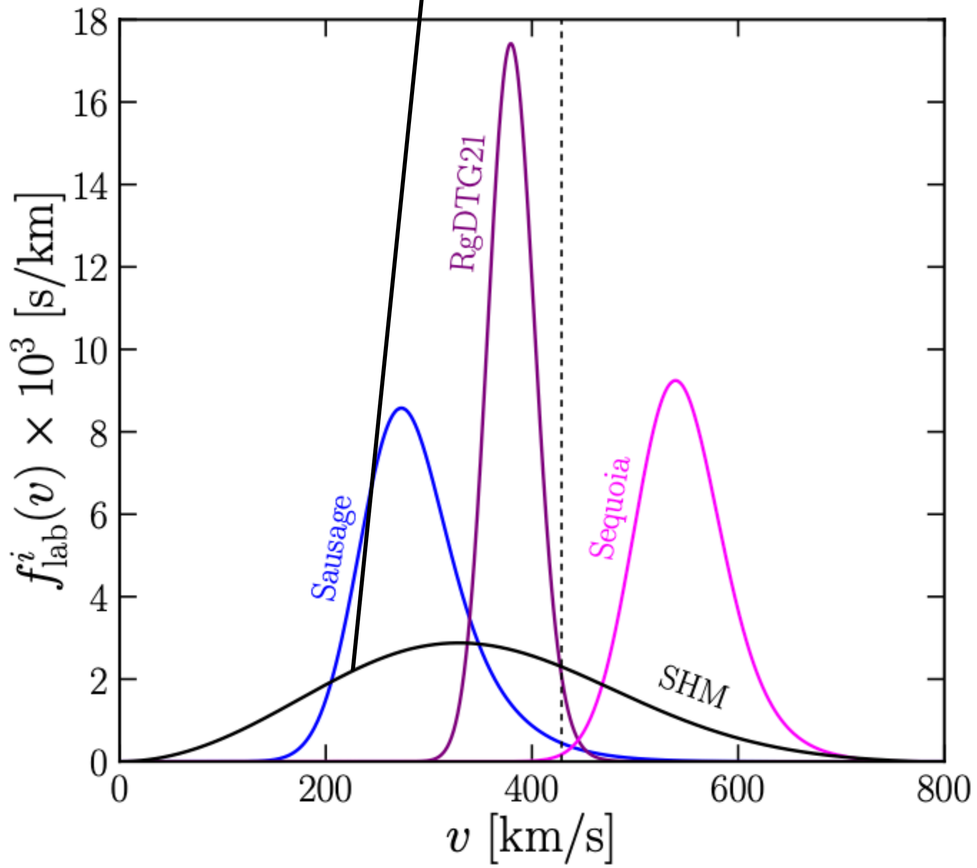

TNM R Laha 2208.14471

DM substructures + SHM

Substructure	Mean velocity (km/s)			Velocity dispersion (km/s)		
	μ_R	μ_ϕ	μ_z	σ_R	σ_ϕ	σ_z
HelmiDTG1	4.5	197.2	244.3	146.0	62.6	42.4
HelmiDTG3	26.2	157.1	-241.3	78.9	28.8	27.2
PolarDTG11	-47.9	21.8	229.2	75.4	19.2	21.5
PgDTG2	221.2	155.7	139.7	26.2	33.8	52.3
Sausage	2.1	-0.3	-8.7	136.6	35.0	72.3
RgDTG28	-4.0	-106.1	-143.2	115.8	29.3	30.3
Sequoia	-36.9	-273.9	-87.0	138.2	36.7	65.0
SHM	0.	0.	0.	155.6	155.6	155.6

$$\frac{dR_{\rm ion}}{d\,ln\,E_e} \propto N_T \frac{\bar{\sigma}_e}{8\mu_{\chi e}^2 m_\chi} \int qdq\,|f_{\rm ion}(E_e,q)|^2\,\rho_\chi\,\eta\left(v_{\rm min}(E_e,q)\right)$$

$$\eta(v_{\rm min}) = \int_{v_{\rm min}}^{\infty} \frac{1}{v}\left[(1-\delta) f_{\rm lab}^{\rm SHM}(\mathbf{v}) + \delta f_{\rm lab}^{\zeta_i}(\mathbf{v})\right] d^3v$$

Substructure fraction

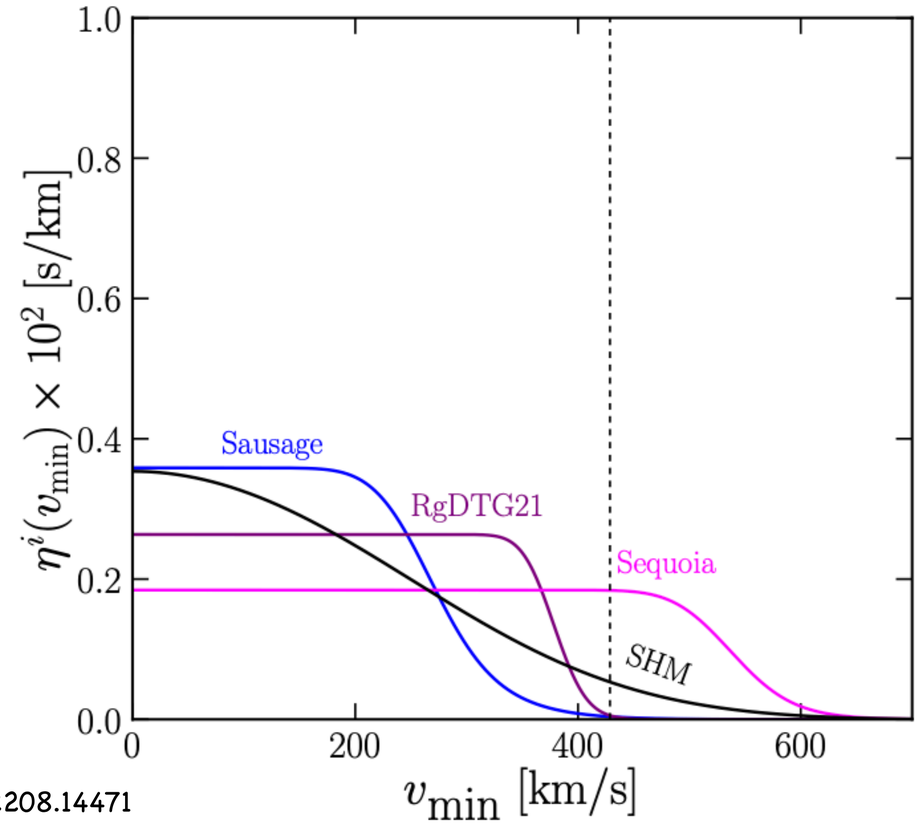

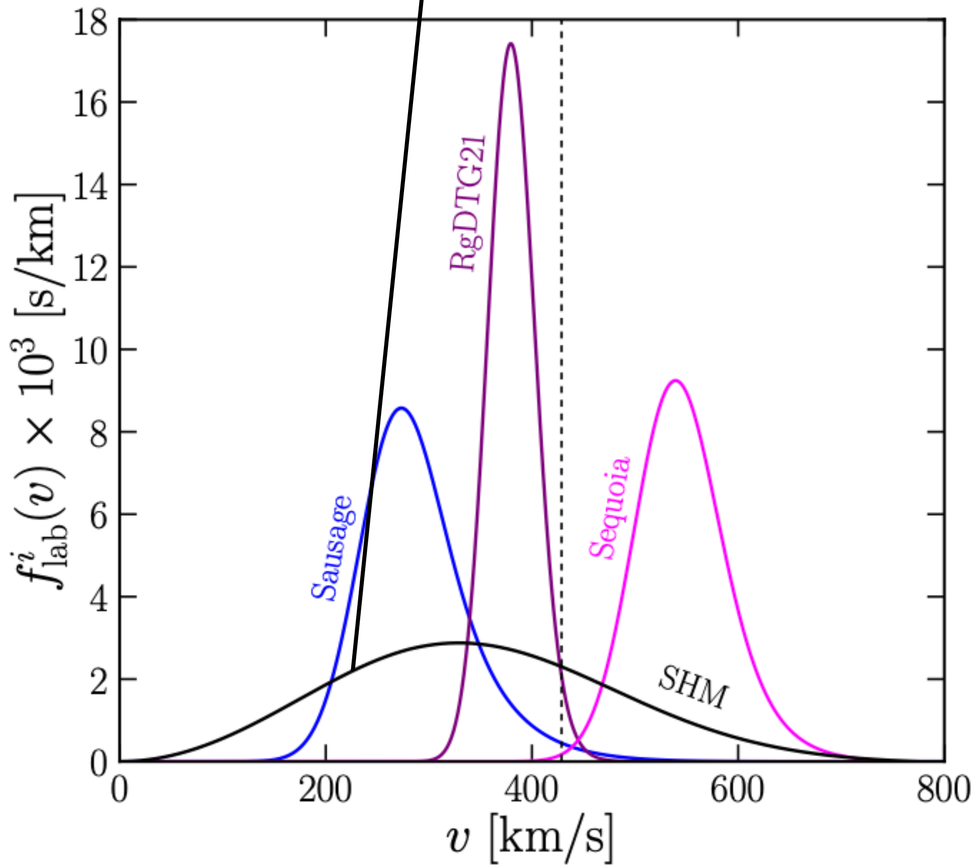

DM substructures + SHM: event rate

$$\frac{dR_{\rm ion}}{d\ln E_e} \propto N_T \frac{\bar{\sigma}_e}{8\mu_{\chi e}^2 m_\chi} \int q dq \, |f_{\rm ion}(E_e, q)|^2 \, \rho_\chi \, \eta\left(v_{\rm min}(E_e, q)\right)$$

$$\eta(v_{\rm min}) = \int_{v_{\rm min}}^{\infty} \frac{1}{v} \left[(1-\delta) f_{\rm lab}^{\rm SHM}(\mathbf{v}) + \delta f_{\rm lab}^{\zeta_i}(\mathbf{v})\right] d^3v$$

Substructure fraction = 1

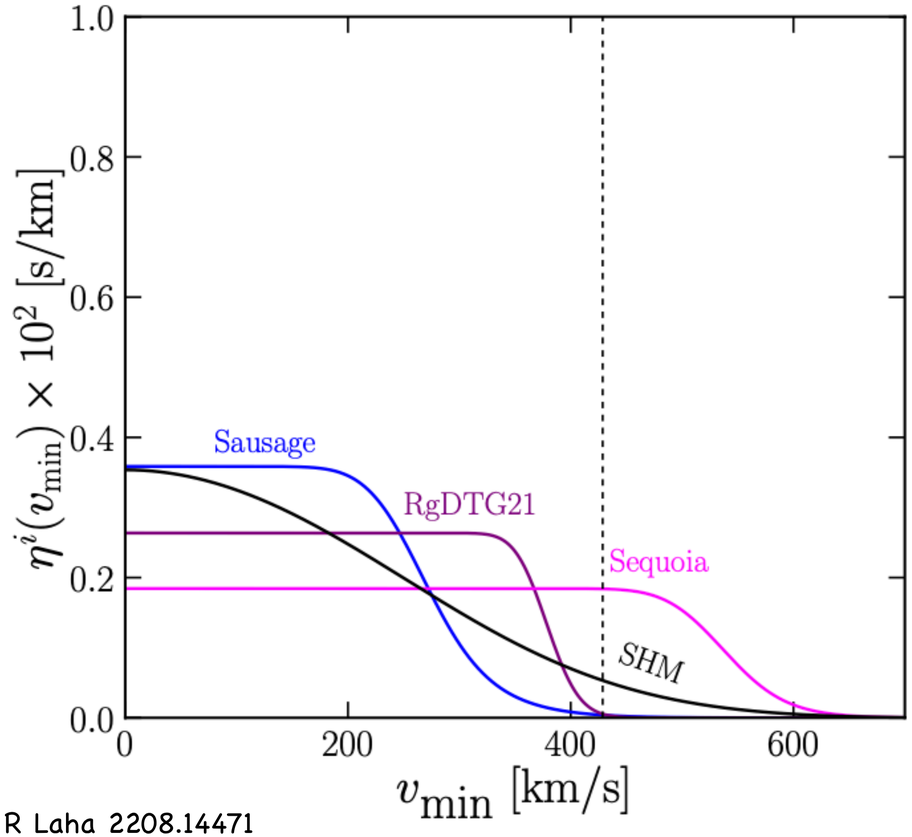

TNM R Laha 2208.14471

DM substructures + SHM: event rate

$$\frac{dR_{\rm ion}}{d\ln E_e} \propto N_T \frac{\bar{\sigma}_e}{8\mu_{\chi e}^2 m_\chi} \int q dq \, |f_{\rm ion}(E_e, q)|^2 \, \rho_\chi \, \eta\left(v_{\rm min}(E_e, q)\right)$$

$$\eta(v_{\rm min}) = \int_{v_{\rm min}}^{\infty} \frac{1}{v} \left[(1-\delta) f_{\rm lab}^{\rm SHM}(\mathbf{v}) + \delta f_{\rm lab}^{\zeta_i}(\mathbf{v})\right] d^3v$$

Substructure fraction = 1

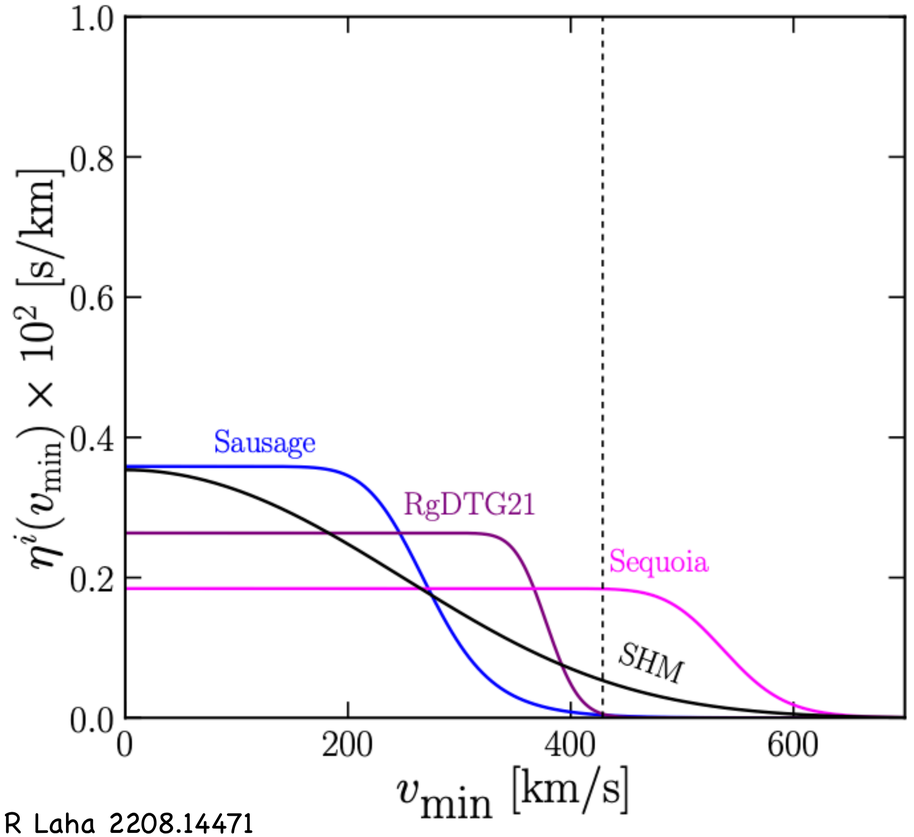

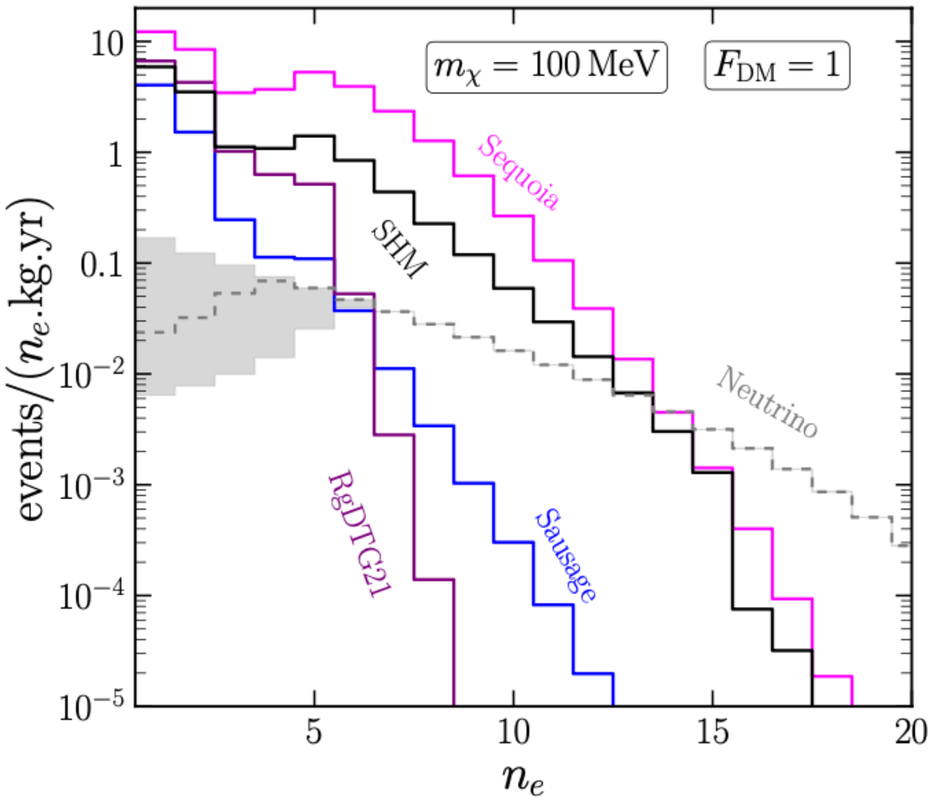

TNM R Laha 2208.14471

DM substructures + SHM: discovery limit

Substructure fraction = 1

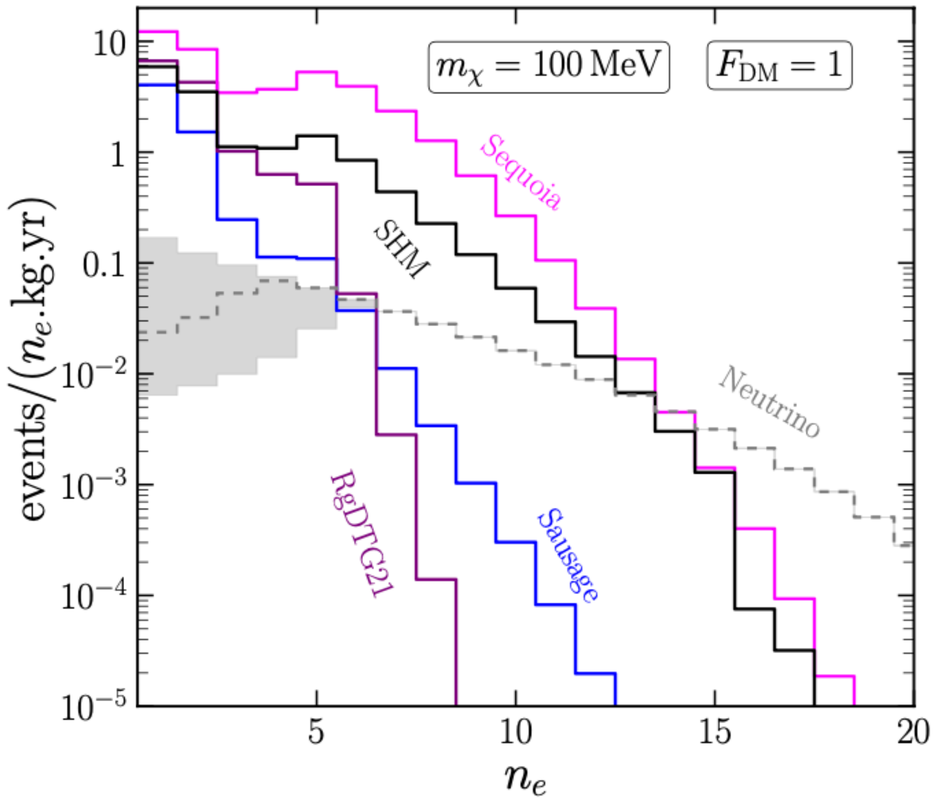

DM substructures + SHM: discovery limit

Substructure fraction = 1

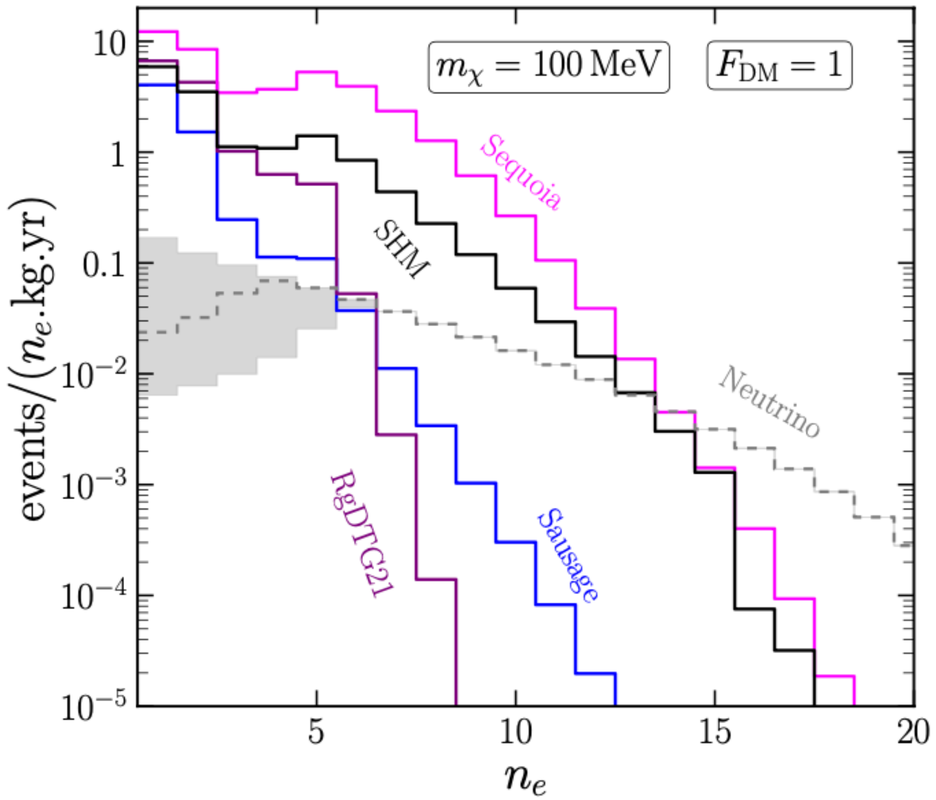

DM substructures + SHM: discovery limit

Substructure fraction = 1

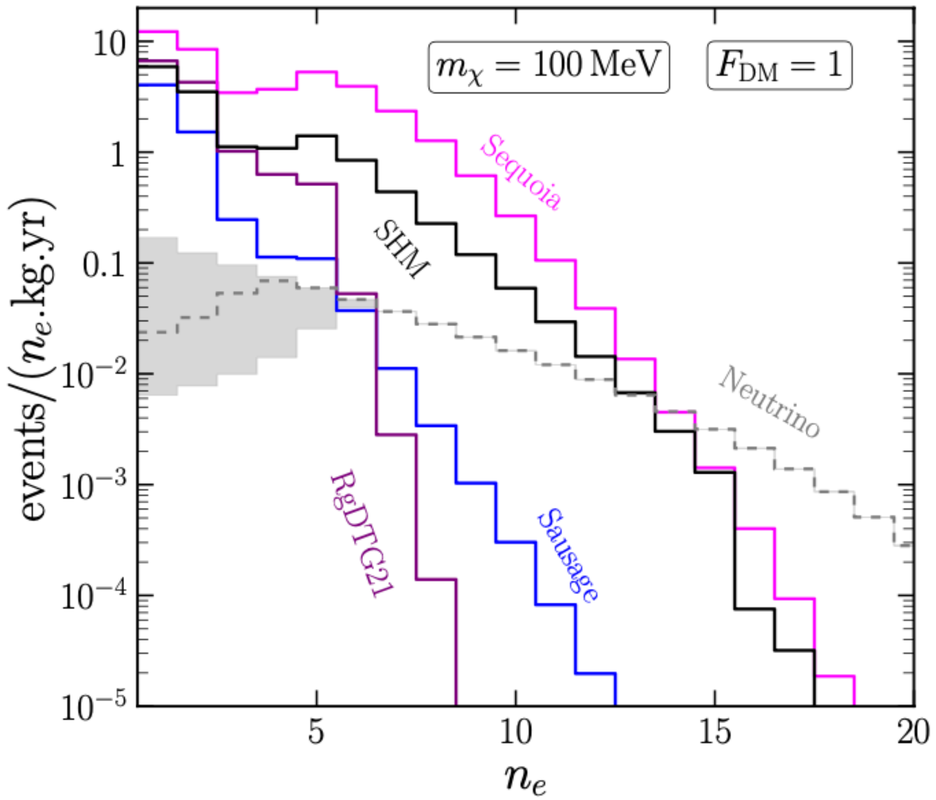

Likelihood analysis

→

DM substructures + SHM: discovery limit

Substructure fraction = 1

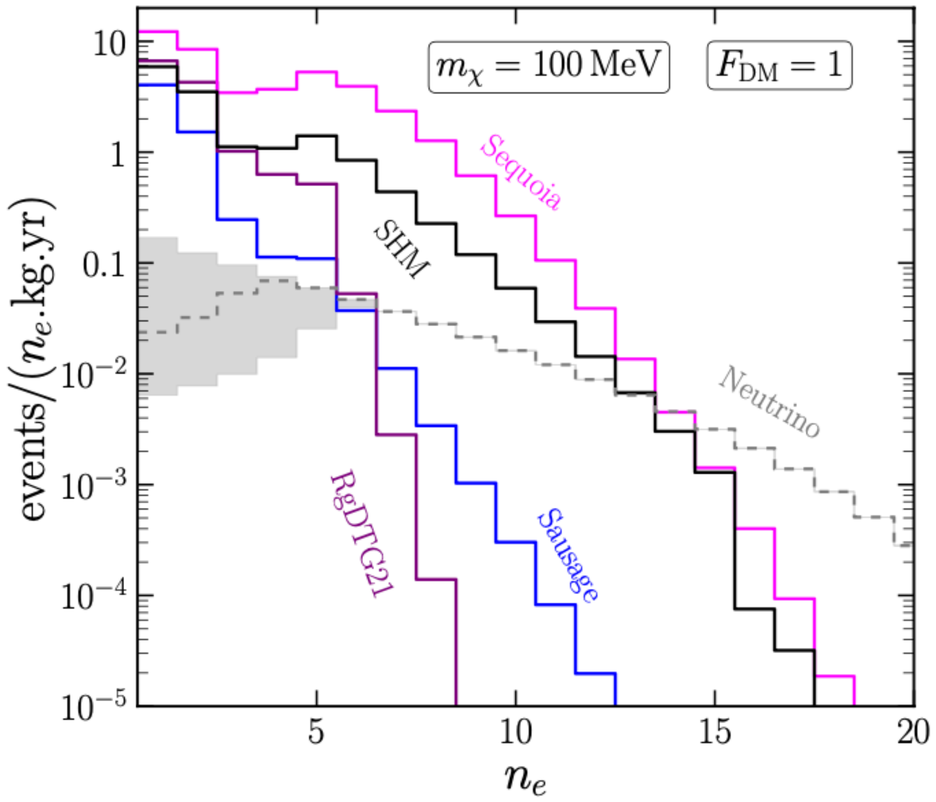

Likelihood analysis

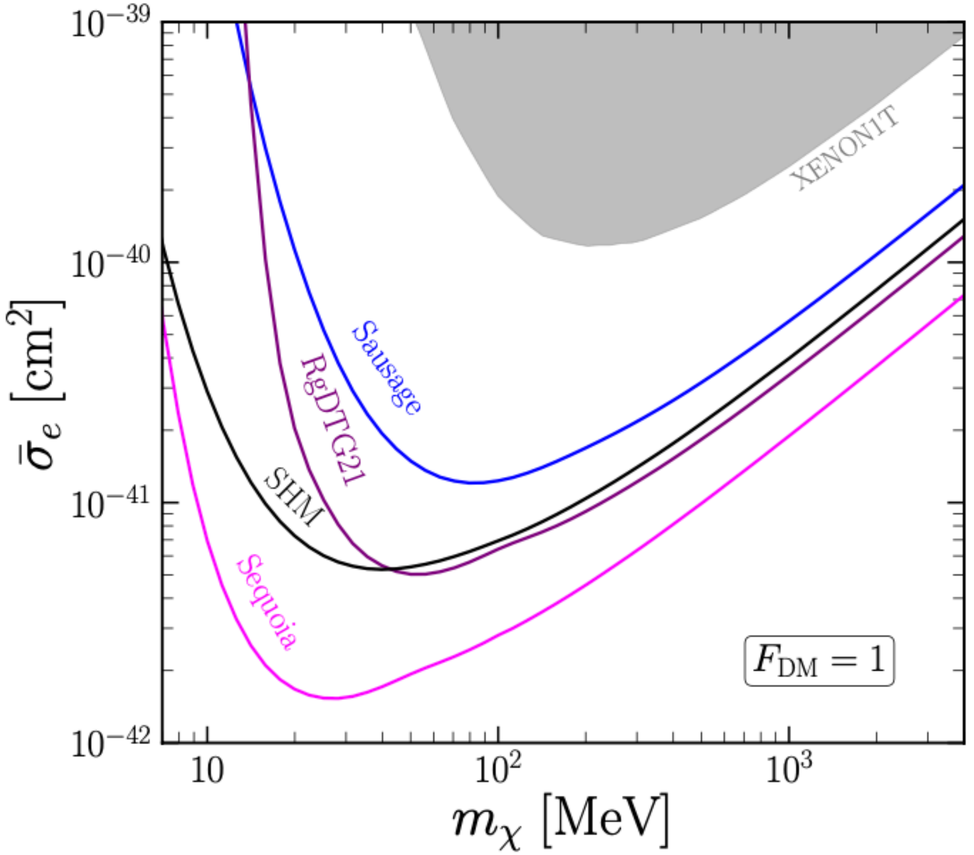

DM substructures + SHM: discovery limit

Substructure fraction = 1

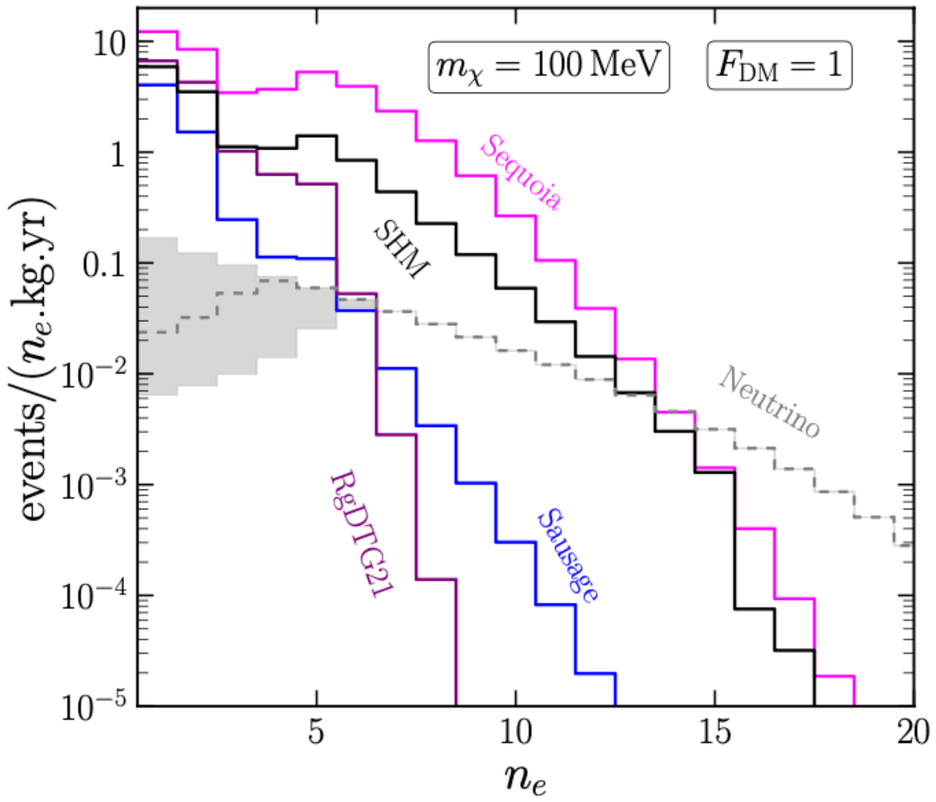

Likelihood analysis

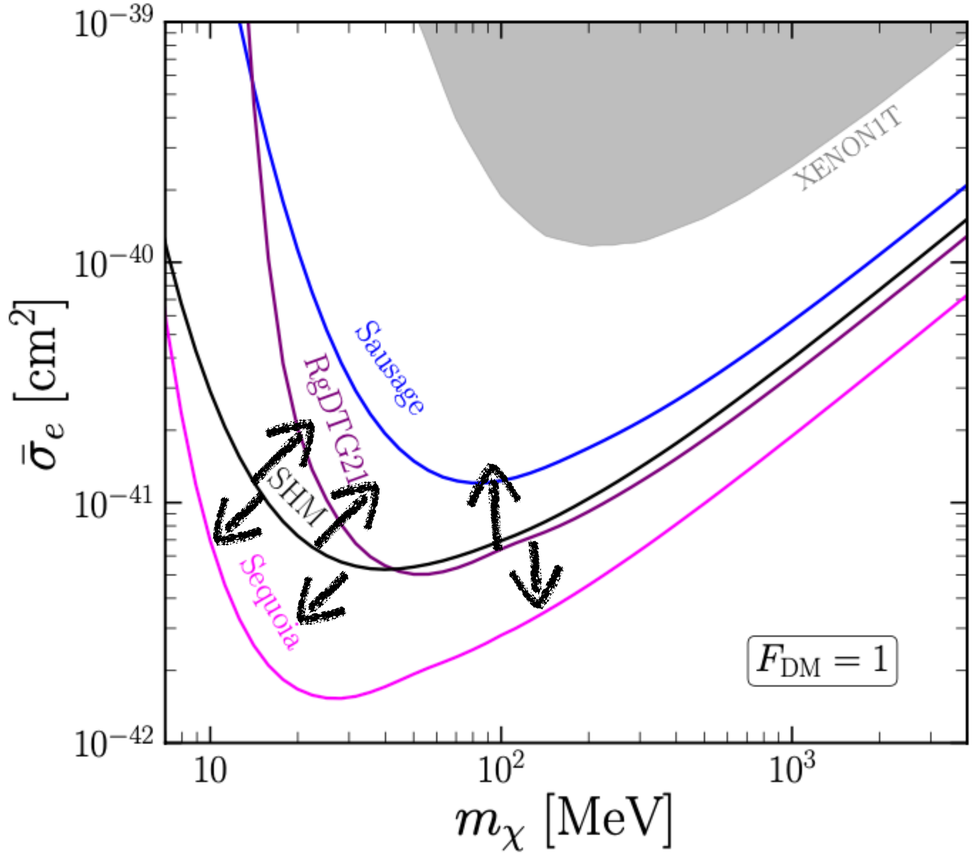

DM substructures + SHM: discovery limit

Substructure fraction = 0.2

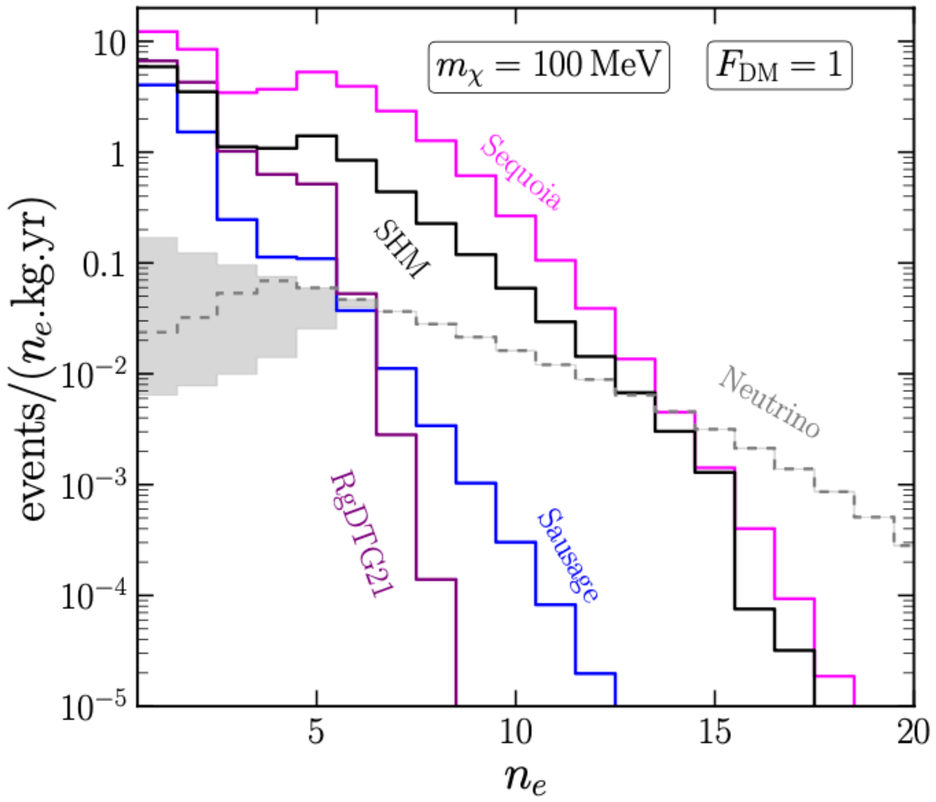

Likelihood analysis

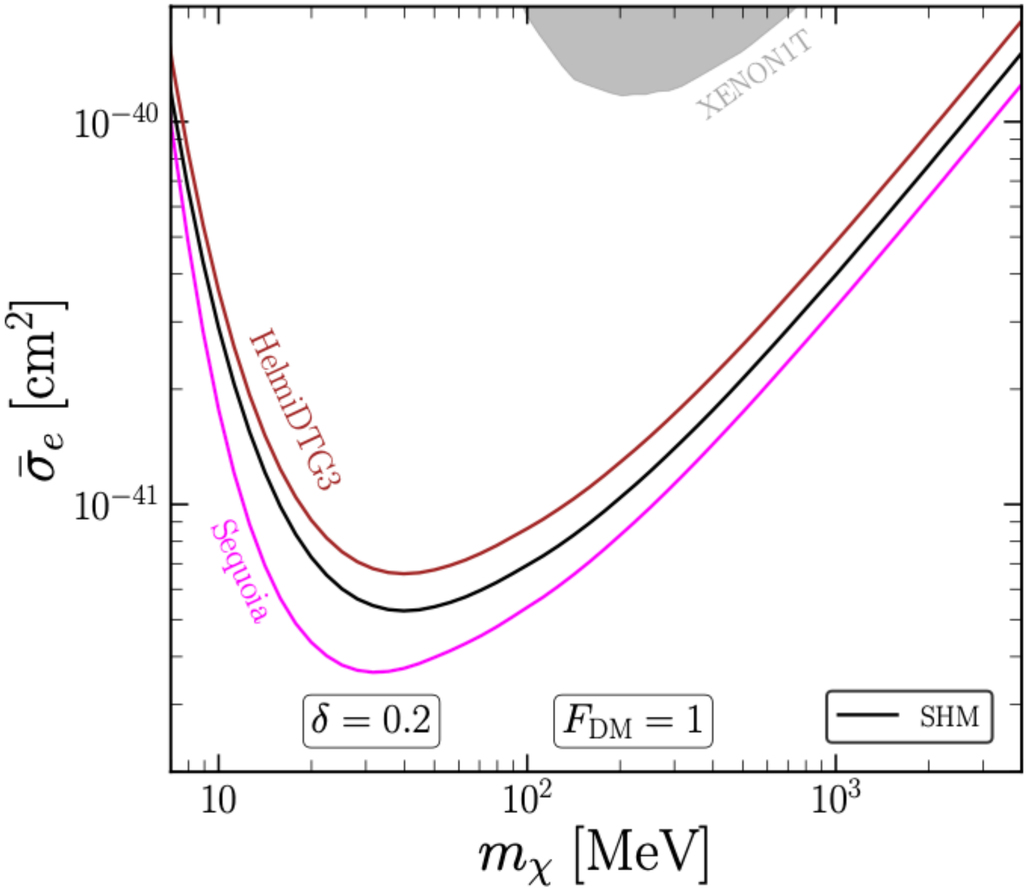

Resolving DM substructure fraction

$$\bar{\sigma}_e = 10^{-40}\,\mathrm{cm}^2$$

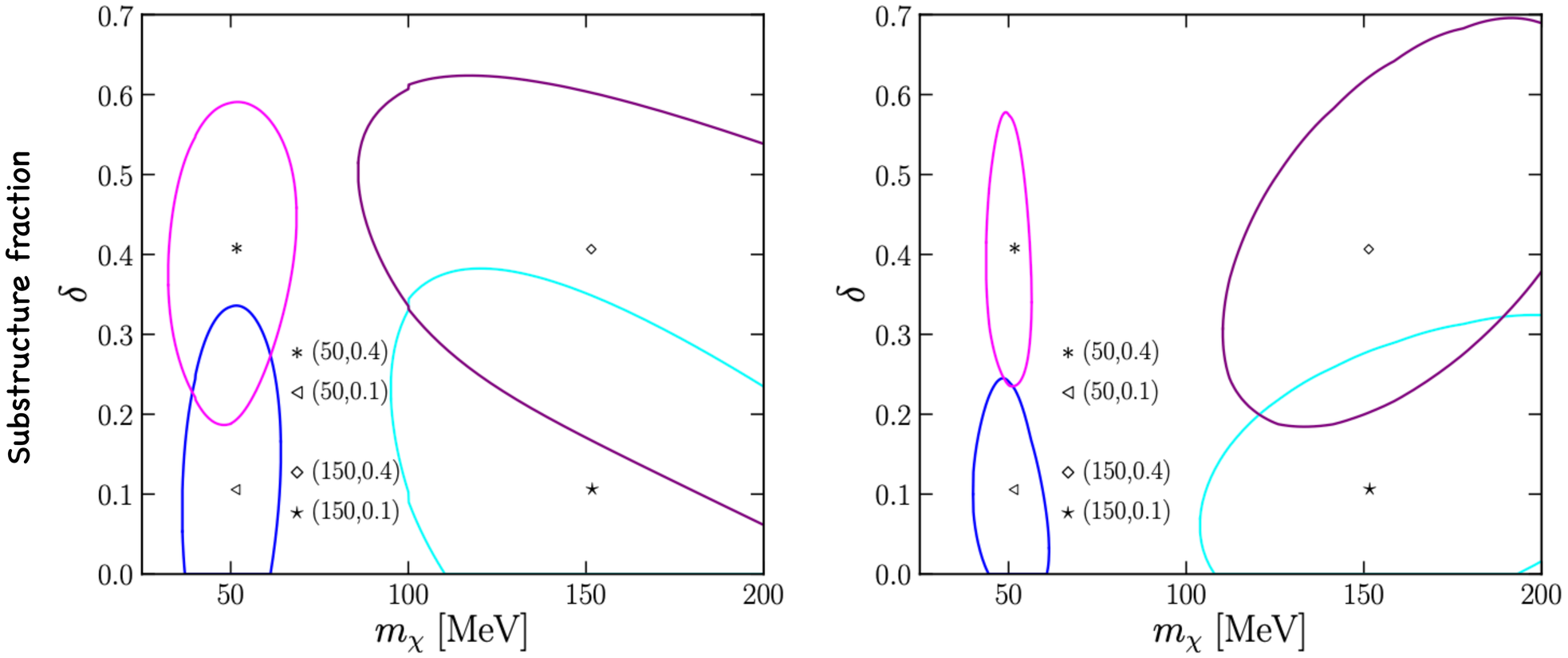

Closed contours for low masses : can be resolved!

Summary

- Clear evidence of stellar substructure!
- Originated from rather recent merger
- The associated DM substructure may have similar velocity distribution?
- Essentially modify local DM speed distribution. How much?
- We explored this effect in electron recoil experiments
- Substructure fraction can be resolved to ~ 50% accuracy...

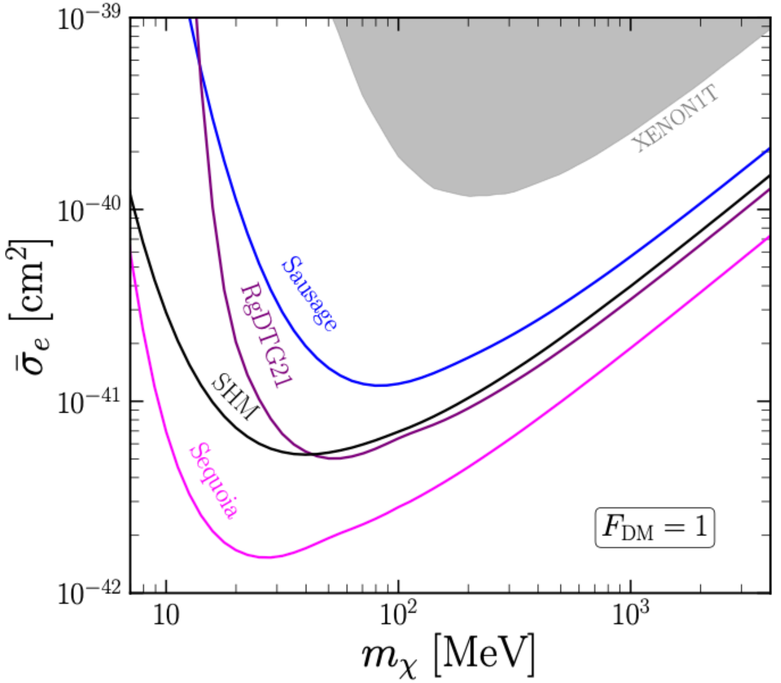

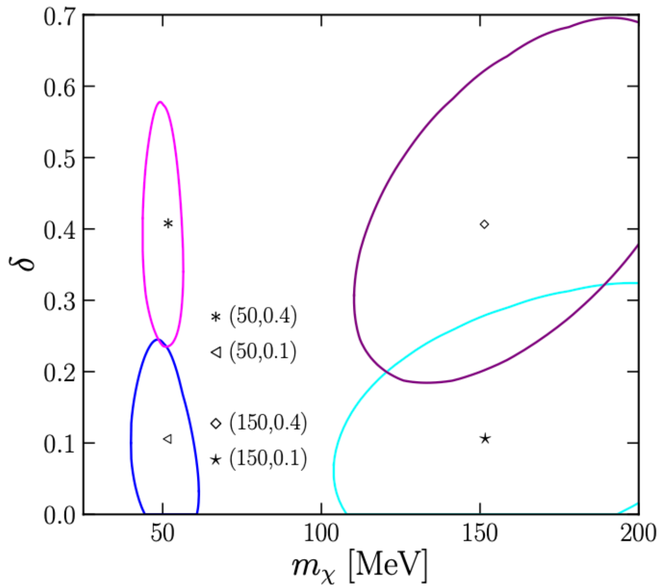

Summary

- Clear evidence of stellar substructure!
- Originated from rather recent merger
- The associated DM substructure may have similar velocity distribution?
- Essentially modify local DM speed distribution. How much?
- We explored this effect in electron recoil experiments
- Substructure fraction can be resolved to ~ 50% accuracy...

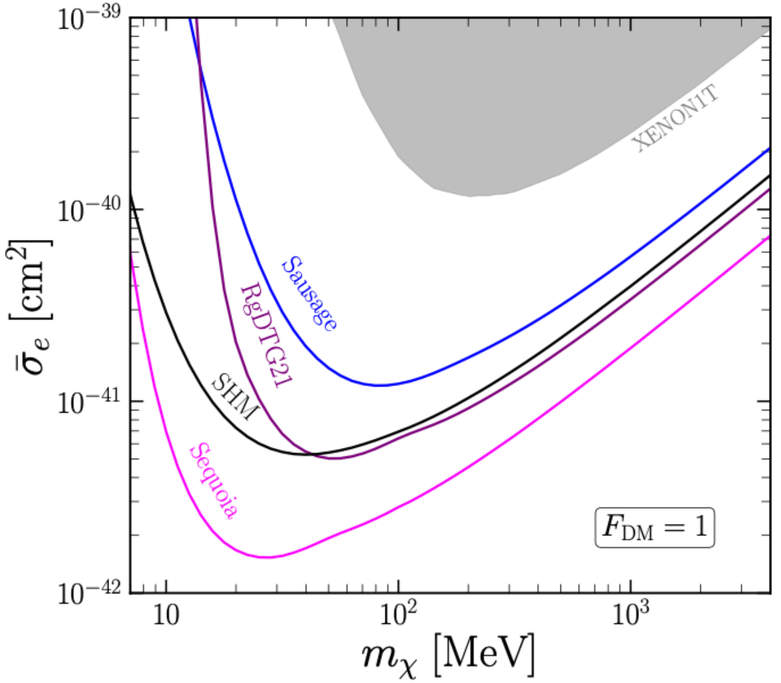

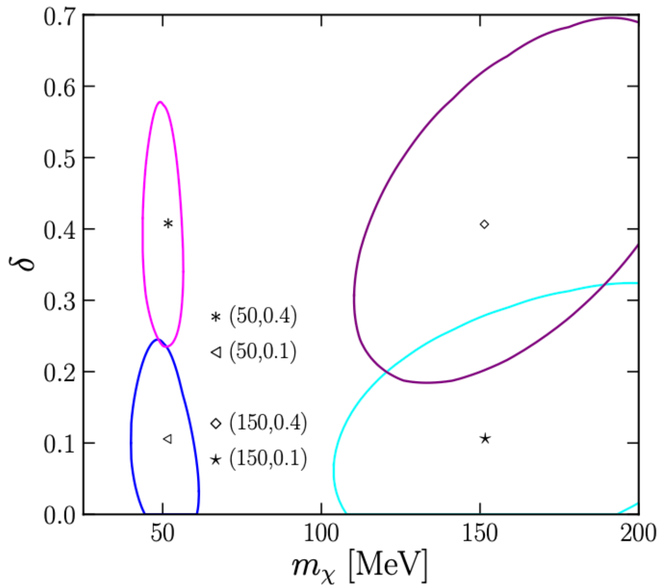

email: tarak.maity.physics@gmail.com

Thank you

TNM R Laha 2208.14471